SLAC Proposal No. E-124
Supplement #2
Received April 18, 1977.

A Three-Photon Measurement of Parton Charge and Search for Color

Submitted by

University of California at Santa Barbara

D. O. Caldwell, A. M. Eisner, C. J. Lauer, A. Lu, and S. J. Yellin

and

University of California at Davis

J. H. Klems, W. T. Ko, R. L. Lander, and D. E. Pellett

April 1977

<u>Contents</u>

I. EXPERIMENTAL GOALS

We propose using a large lead-scintillator shower detector of novel design and an alternation between e^+ and e^- beams to measure the difference between $e^+p \to e^+\gamma X$ and $e^-p \to e^-\gamma X$ in order to (1) provide a crucial test of the parton model, (2) determine whether partons have fractional or integral charge, (3) in the latter case determine whether these are Han-Nambu colored quarks or are of the Pati-Salam type, and (4) provide information on valence parton distribution functions, uncomplicated by the parton-antiparton or gluon effects.

Simultaneously with this primary measurement we would obtain information on π^o and η electroproduction and a precision comparison of e^+ and e^- inelastic scattering at large values of the four-momentum transfer. An auxiliary measurement using a photon beam would provide important checks on the data obtained with the electron beam and would in addition give information on π^o and η photoproduction, and on the existence of any high-mass particles which decay into photons, electrons, or π^o's.

The Santa Barbara group has performed a 200-hour trial (E-99) of this experiment, which will be discussed in Section III and is described in more detail in the appendix (which reproduces papers which appeared in the 15 November 1976 Physical Review Letters[1] and will appear in the 11 April 1977[2] issue of that journal). The main result is that despite finding no difference in e^+ and e^- inelastic scattering to good accuracy ($e^+/e^-=1.0027 \pm 0.0035$, including statistical and systematic effects), we did observe a difference between $e^+ + p \rightarrow e^+ + \gamma +$anything and $e^- + p \rightarrow e^- + \gamma +$ anything, getting $e^+/e^- = 1.080 \pm 0.036$. This difference is of the right sign and magnitude according to the parton model calculations of Brodsky, Gunion, and Jaffe.[3] In fact, using that model the results yield a mean sum of parton charges cubed in the proton, $\langle \sum_i Q_i^3 \rangle = 0.89 \pm 0.34$. Statistics are insufficient to distinguish among fractional charge ($\langle \sum_i Q_i^3 \rangle = 0.56$), integral charge ($\langle \sum_i Q_i^3 \rangle = 1$), integral charge for colored quarks below the color threshold ($\langle \sum_i Q_i^3 \rangle = 0.78$), or the somewhat lower value for Pati-Salam quarks.

In order to discuss the goals of the primary measurement further, one needs more information on the theoretical background of this $e^+ - e^-$ difference determination, and this is done in the next section. The rest of the present section will be devoted to discussion of the secondary goals of the experiment.

Our previous[1] comparison of $e^+ - e^-$ inelastic scattering from protons covered the range of virtual photon kinematics, $1.2 < |q^2| < 3.3$ $(\mathrm{GeV}/c)^2$, $2 < \nu < 9.5$ GeV, in four-momentum transfer squared and energy, respectively. The observed lack of two-photon exchange effects to this level of accuracy is perhaps surprising, but in addition this result has two consequences for the main experiment: (1) two-photon interference effects are unlikely to be responsible for the difference (of about 8%) we observed in the real photon production channel, and (2) this provides proof of no experimental biases in the e^+ and e^- detection which could affect the difference we observe in γ production.

In the proposed experiment we would obtain simultaneously with the photon production data an extension of the accurate comparison of e^+ and e^- deep inelastic scattering to $3<|q^2|<10\,(\mathrm{GeV}/c)^2$ where differences are more likely to appear. In that higher range of q^2 the accuracy of the measurement should exceed our previous effort. Besides better statistics, systematic errors which result from the beam location and halo will be reduced. The beam location accuracy will not only be improved with a microwave beam centering device, but also the proposed symmetric apparatus will be much less sensitive to this error. Perhaps at last some two-photon exchange effect will be seen.

We have just finished the analysis of another experiment (E-88) done contiguously with E-99 and performed with the same apparatus, but done in a different kinematic region so as to measure deep inelastic π^o electroproduction. The results can be interpreted as providing further information on the parton structure of the photon and of the proton. For instance, the electroproduced π^o's have a mean transverse momentum which becomes independent of $|q^2|$ in the range of 2 to 8 $(\mathrm{GeV}/c)^2$ and of a value like that found in hadronic processes. The longitudinal momentum distribution is also quite similar to that found in e^+-e^- annihilation or in hadronic collisions. Both results are consistent with the virtual photon's interacting with a parton, which then produces a hadronic "jet", the nature of which is independent of the incident particle. This is unlike the behavior we found for real photons (in π^o photoproduction[4]) which appear (in at least one kinematic region) to dissociate into a parton-antiparton pair, which subsequently interact with partons in the nucleon to produce two "jets". Substantiation of the above picture of virtual photon-parton interactions is provided by the flat π^0 azimuthal dependence, the π^0 cross section's being close to the average of the π^+ and π^-, and by the dependence of the π^0 cross section on center-of-mass energy.

The experiment proposed here, unlike our previous one, would permit a simultaneous measurement of π^0 electroproduction in an interesting kinematic region. In fact, it would have both a considerably increased efficiency for π^0 detection and an increased kinematic range, particularly permitting measurements farther into the deep inelastic region. This would provide an extension of the previous work in accuracy, as well as in q^2 and transverse momentum. Tests not previously possible would become feasible, such as detailed comparisons with the Constituent Interchange Model, and a possible way to measure the transverse momentum distribution of partons in the proton. Another interesting possibility is a more direct comparison between the interaction of real and virtual photons over a similar kinematic range, since we would plan to spend about 100 hours using a photon beam, mainly for checks having to do with the primary goal of the experiment. However, this would also provide π^0 and η^0 photoproduction data over a larger kinematic range than we achieved in a previous SLAC experiment[4] (E-76). (We might also be able to check out to larger values of transverse momentum our previous[5] result of an extraordinarily large deep inelastic Compton scattering.)

The photon beam run could in addition provide an interesting search for high-mass particles which decay into photons, electrons, or π^0's. We ought to be able to get up to masses approaching SLAC's kinematic limit (~5 GeV/c^2). In 100 hours we could get down to ~10^{-4} of the $\psi \to e^+ + e^-$ cross section, so the search could be a rather definitive one. Since part of SLED will be operational soon, with reduced beam intensity and SLED we could extend this search to even higher masses, but that would require a separate run with a smaller target-to-detector distance.

II. THEORETICAL BACKGROUND FOR THE $e^+ - e^-$ DIFFERENCE MEASUREMENT

Brodsky, Gunion, and Jaffe[3] suggested that a difference could arise between the e^+ and e^- cross sections for deep inelastic electroproduction of photons from an interference between the Bethe-Heitler bremsstrahlung amplitude and the virtual Compton amplitude. These two processes are shown in Fig. 1.* If the proton is considered to be made of partons, it is seen from these diagrams that one photon interacts with a parton in the Bethe-Heitler case and two photons interact with a parton in the Compton case, so that in taking the square, the interference term (Fig. 1c) is effectively a three-photon interaction with the parton. The interference or difference term then has odd charge conjugation and depends on the cube of the parton's charge.

Specifically, the difference of the positron and electron cross sections in the deep inelastic region determines a structure

---

*To ensure being in the deep inelastic or scaling region, reference 3 suggests having $|q^2|>1$ and $|\tilde{q}^2-q^2|>1$ in units of $(\mathrm{GeV}/c)^2$.

function* which in the parton model has the form

$$V(x) = \sum_a \lambda_a^3 U_a(x), \qquad (1)$$

where $U_a(x)$ is the probability of finding a parton of type "a" with charge λ_a and fraction x of the proton's momentum in an infinite momentum rest frame. See Eq.(1) of the second article in the Appendix and the subsequent discussion for the relationship between V and the cross section difference. Note that in the parton model V depends on only one (x) of the six kinematic variables needed to specify the process. This scaling with x alone provides a very stringent test of the parton model and checking just this feature would be sufficient justification for the experiment.

Furthermore the measured V(x) helps determine $U_a(x)$, which has been sought in inelastic electron, muon, and neutrino experiments. In principle the present experiment is the cleanest way to determine the valence quark part of $U_a(x)$. Because of the odd charge conjugation there are no Pomeron contributions arising from the quark-antiquark sea in this process. Thus this experiment ought to shed further light on the behavior of valence quarks, provided V(x) scaling is observed. It could provide a test of p-quark dominance without the ambiguities of the inelastic electron scattering from deuterium.

---

*This is the combination of longitudinal and transverse structure functions. In subsequent calculations we use a combination appropriate to parton spin 1/2.

If one could measure over all x values from 0 to 1, then the parton charge could be determined without any knowledge of $U_a(x)$ by using an exact sum rule. The point is that $Q=\int_0^1 dx \sum_a \lambda_a U_a(x)$, $Y = \int_0^1 dx \sum_a y_a U_a(x)$, and $B = \int_0^1 dx \sum_a b_a U_a(x)$ are the charge, hypercharge, and baryon number of the target particle of interest, and because it has odd charge conjugation, λ_a^3 can be reduced to a linear combination of λ_a, y_a, and b_a. Thus the integral $\int_0^1 V(x)dx = \int_0^1 dx \sum_a \lambda_a^3 U_a(x)$ is determined just by quantum number conservation. If the parton charge is 0 or ±1, $\lambda_a^3 \equiv \lambda_a$, so

$$\int_0^1 V(x)dx = Q = \begin{cases} 1 \text{ for protons} \\ 0 \text{ for neutrons} \end{cases}, \qquad (2)$$

and for fractionally charged quarks, $\lambda_a^3 = \frac{1}{3}\lambda_a + \frac{2}{9} b_a$, so

$$\int_0^1 V(x)dx = \frac{1}{3} Q + \frac{2}{9} B = \begin{cases} 5/9 \text{ for protons} \\ 2/9 \text{ for neutrons} \end{cases}. \qquad (3)$$

Note that an even charge conjugation process, such as inelastic electron scattering, does not lead to an exact sum rule for the charge. Furthermore, if neutral gluons are present, the inexact sum rules obtained give an erroneously low charge value. The three-photon process considered here is completely insensitive to the presence of gluons.

Chanowitz[6] has added an exciting new reason for doing this experiment, the possible direct detection of "color". Below the color threshold the electromagnetic current has only color singlet interactions, and hence quarks would display fractional charge.

However, in the Compton amplitude, where the current comes in as the square, there is a color octet contribution to intermediate states. The existence of color is then shown by the increase in the mean cubed charge, resulting (for protons) in

$$\int_0^1 V(x)\,dx = 7/9 \ , \tag{4}$$

for integrally charged Han-Nambu quarks below the color threshold. This, then, is a specific and very important reason for doing this experiment at SLAC energies.

Pati[7] has informed us that gauge-integer-charged quarks would be expected to yield a value for (4) which is also between the values for fractional and integral charges, but different from 7/9. It is expected that a detailed calculation of this will be done soon, permitting at least in principle the experimental distinction by this kind of an experiment of gauge and Han-Nambu integrally charged quarks.

However, the sum rule for V(x) suffers from the same problem similar quark sum rules do, namely that most partons have small x values, and it is difficult to make measurements to small enough values of x. In the small x region there can be a Reggeon-exchange contribution with an integrable $x^{-1/2}$ singularity. One can obtain[8] a limit on the contribution to $\int V(x)dx$ from the large x region by noting that

$$\nu W_2^{ep}(x) = x \sum_a \lambda_a^2 \, U_a(x) \tag{5}$$

and getting an upper bound from assuming that only the p (or up) quark contributes with its charge of + 2/3. Thus

$$\frac{2}{3}\int_{x_o}^{1} \frac{\nu}{x} W_2^{ep}(x)\,dx > \int_{x_o}^{1} V(x)\,dx. \qquad (6)$$

The measurable lower limit, x_o, depends on how small a value of q^2 (see Fig. 1) one can use and still get scaling, and only the experiment can determine that. However, $x_o = 0.05$ is an absolute limit, and if $x_o = 0.15$, then >54% of $\int_0^1 V(x)dx$ is not measurable,[8] if the whole integral is equal to 5/9. Thus there are two ways to do the experiment: (1) measure to sufficiently small x so that the data can be extrapolated to x = 0, knowing the $x^{-1/2}$ dependence, which is fortunately possible because there can be no x^{-1} Pomeron contribution; or (2) use the larger x region where the quark charge is given from the ratio of V(x) to $\nu W_2/x$ to a good approximation. The inelastic scattering results (eq. 5) depend on λ_a^2, and the difference experiment (eq. 1) depends on λ_a^3, so the ratio determines λ_a (particularly for p-quark dominance) in a sense to be more fully defined in the next paragraph. While both approaches will be used, the second is more certain of success and has the advantage that one is dealing primarily with the ratio of two experimental results, with relatively little theoretical uncertainty. If the parton charge is integral, the bound of eq. 6 would be exceeded.

This method of determining the type of partons which exist in the proton is illustrated in Fig. 2, where the ratio, $R = \frac{V(x)}{\nu W_2/x}$, is given versus x for various assumed forms of V(x). If the proton consisted of only valence quarks of fractional charge, then one would measure the curve labeled $\frac{11}{15} - \frac{4}{15} \frac{\sigma^N}{\sigma^P}$, where σ^N and σ^P are respectively the cross sections for inelastic electron scattering for neutrons and protons. However, inelastic electron scattering is affected by the quark-antiquark sea, so if that effect is put in, the measured curve becomes the one labeled $\frac{V(x)}{\nu W_2/x}$. The error bars on that curve refer to this experiment's capability for determining that curve, and they will be discussed later. If the proton consisted of p quarks alone, then R is given by the line "Fractional Upper Bound," which is then the absolute maximum value of R which fractional charges could give. Above this lies a curve labeled $\frac{17}{15} - \frac{8}{15} \frac{\sigma^N}{\sigma^P}$, which is the curve for R which would result if there were only valence quarks of the colored, integrally-charged Han-Nambu type, and the measurement is made below the color threshold. The effect of having these quarks can best be judged by comparing this curve with the first one described above, since the same assumption about no quark-antiquark sea is made in both cases. Corrections for non-valence quarks are expected to be negligible for large x and of the order of magnitude illustrated for small x.

III. PREVIOUS EXPERIMENT (E-99)

Using apparatus (Fig. 3) originally designed for an experiment (E-88) on deep inelastic π^0 production, the UCSB group used 200 hours of accelerator time to check out and try the three-photon experiment. As can be seen from the figure, there was a stack of 88 lead glass counters (of 2 1/2" x 2 1/2" cross section) on one side of the 13.5-GeV e^+ or e^- beam, and a scattered electron detector on the other side. The electron detector consisted of a bending magnet and a hodoscoped lead and scintillator shower detector, which could be moved into the main beam for calibration. The electron and photon detectors had acceptances of 3.1 msr and 8.8 msr, respectively. Further information on the detectors and on charged pion contamination in the electron detector (2-3%, measured in three independent ways) is given in the Appendix.

Although a wider range was covered in E-88 by having a higher beam energy and moving the detectors, in E-99 we used a single position and detected electrons such as to give virtual photons of $|\tilde{q}^2|$ from 1.2 to 3.3 $(\mathrm{GeV}/c)^2$ and ν from 2 to 9.5 GeV. Interleaved e^+ and e^- data were collected in equal amounts at three beam intensities (3×10^7, 5×10^7, and 7×10^7 e's/pulse), so that any rate-dependent effects could be monitored. This did not produce any important systematic errors in even the e^+-e^- inelastic scattering difference, nor did beam integration differences with e^+ and e^-, beam diameter differences, beam angle error, quantameter errors, magnetic effects on phototubes, or high-energy δ-rays. In the single-arm experiment, where the statistical error was 0.25%, four sources of systematic error each contributed about 0.1%. One was due to inaccuracies in the correction for pion contamination, there being more π^+ than π^-. Another arose from the lack of reproducibility of the incident beam position; this setting error of about 0.5 mm was random, but it left a residual error. The third was from beam halo differences and could be measured in target-empty runs. The fourth was the limit which could be placed on the accuracy of setting the magnetic field for the two polarities. All of these can be improved or eliminated in the proposed experiment, and all will be unimportant for the e-γ measurements.

For the photon detection experiment, all photons in time coincidence with a suitable electron and having an energy greater than 4 GeV had their pulse heights and arrival times recorded, and all accompanying particles yielding more than 1 GeV were also recorded. With this information, it was relatively straightforward to make good corrections for accidental coincidences, although in principle if one were careful (as we were) to use the same beam intensities, these should subtract out in the e^+-e^- difference. Where the difference subtraction was really important was in eliminating the background from $\pi^0 \rightarrow 2\gamma$ decays. That this subtraction was being done correctly could be checked by measuring simultaneously the amount of π^0 production by analyzing those cases in which both photons had sufficient energy to be counted. Within statistics, the number of π^0's produced by e^+ and e^- were the same. It is important to note that <u>all</u> spurious hadronic processes (even the decay of presently unknown particles) must subtract out in this difference.

The result of the e^+ and e^- deep inelastic scattering comparison has been given above. Although that difference was less than 1/3% we did observe a difference in the channel in which an energetic photon was produced, getting $\frac{e^+ \rightarrow \gamma}{e^- \rightarrow \gamma} = 1.080 \pm 0.036$. In principle the mean cube of the parton charge could then be determined through integrating over V(x), which is given (see Appendix) by

$$V(x) = \frac{2\pi^2 M_p p_o(-q^2)}{\alpha^3 |T_{int}|^2} (\sigma_+ - \sigma_-), \qquad (7)$$

where $\sigma_\pm = \dfrac{d^6\sigma(e^\pm p \to e^\pm \gamma X)}{\frac{d^3p'}{p_o}\frac{d^3k}{k_o}}$, the various kinematic quantities are defined in Fig. 1 (with the subscript 0 indicating the energy part of the corresponding four-momentum), and $|T_{int}|^2$ is a <u>known</u> electrodynamic function arising from the interference of the Bethe-Heitler and Compton amplitudes. However, the small-x problem discussed in the previous section makes the charge determination model dependent, because the data neither goes to very small x nor has good enough statistics. The result of this short run is a mean-cubed charge of 0.89±0.34, where the errors are statistical and do not include the uncertainty in extrapolating to small x values. While this result does not distinguish between the various charge possibilities we have discussed, the observation of the right sign and magnitude of the effect is a confirmation of the theoretical ideas and calls strongly for further measurements. Further details on the E-99 experiment can be found in the Appendix.

IV. RATES, BACKGROUNDS, AND STATISTICAL PRECISION

A. General Philosophy

In order to test adequately the parton model for the three-photon process and to separate the various predictions for parton charges, we require that the variances for the integrals discussed in Section II be about 50 times smaller than in E-99. Roughly speaking, this implies we need about 50 times more events in the relevant kinematic regions. While some of this can come from an increase in running time, a large solid angle detector is clearly indicated. The approach and detector we are proposing will be able to achieve $\approx$ 5% statistical precision in 100 efficient hours per polarity, assuming 180 pps and 10^8 20 GeV $e^{\pm}$/pulse on a 5 inch liquid hydrogen target. The large solid angle probably also permits the explicit identification of a majority of π^o background events. We have not, however, included this potential gain in our statistical summaries.

Our first thought was to expand the separate electron and photon detectors of E-99, continuing to use a magnetic spectrometer on the electron side, and perhaps also using the magnet to sweep low-energy charged particles away from the photon detector. However, not only is it difficult to achieve a large solid angle in this manner at a reasonable cost; but even stray fields on the photon side can lead to spurious asymmetries of a sort very difficult to correct for. The difficulty is that charged pions sometimes simulate lower-energy electromagnetic particles in shower detectors, and that the numbers of π^+ and π^- are unequal. When the magnet polarity is reversed (to switch between e^+ and e^-), the directions in which the $\pi^{\pm}$ are swept would also be reversed, and an asymmetry (significant relative to our intended precision) would result. (A magnet powerful enough to sweep all $\pi^{\pm}$ away from the photon detector is not feasible.) Other asymmetries could result from sweeping low-energy $e^{\pm}$ backgrounds into the detector and from small fringe field effects on the photon detector's phototubes. On the other hand, restricting the field entirely to the electron side seems extremely difficult if one wants a large solid angle and a non-astronomical price tag.

We have therefore turned to a single large non-magnetic electron-photon detector, with a central hole for the beam. This allows detection of both electrons and photons over all azimuthal angles, as well as over a large range of polar angles. The specific detector to be described covers a solid angle of 0.18 sr, leading to an uncorrelated two-particle acceptance approximately 1000 times larger than in E-99. This arrangement eliminates the troublesome magnet-associated systematic errors, and the symmetry greatly reduces other systematic errors, such as those due to beam steering.

The novel property of this detector is that no attempt is made to distinguish electrons from photons. For single particle measurements (or for a coincidence measurement in which the second particle is identified as a π^0), kinematic cuts can select a fairly clean sample of electrons. For the e-γ coincidence measurement one must measure the sum of the rates for both possible identifications. The four-momentum transfer q to the nucleon depends only upon the sum of the momenta of the detected particles. Thus the important variables for the process of Fig. 1, q^2 and x, are invariant under the interchange of the particles. Hence the measured asymmetry will in the parton model be proportional to

$$\left[|T_{int}(e\gamma)|^2 + |T_{int}(\gamma e)|^2\right]V(x)$$

where the two known (electrodynamic) functions T_{int} are to be computed for the two possible identifications. One must apply cuts so that the scaling region[3] criteria $|q^2|>1$ GeV^2, $|q^2-\tilde{q}^2|>1$ GeV^2 and (implied by these) $|\tilde{q}^2|>2$ GeV^2 are satisfied for both possible values of $\tilde{q}^2$. It then turns out that the two interference terms almost always enter with the same sign in the regions of interest. (Despite the notation, $|T_{int}|^2$ can be a negative quantity.)

Of course, it is true that one must now consider backgrounds of the types ee, γe, and $\gamma\gamma$ as well as eγ. However, the resulting decrease in signal-to-noise is not an important drawback, especially in light of the enormous increase in solid angle this detector provides.

We have chosen to cover polar angles from approximately 6°–15°. For smaller angles, few events satisfy the cuts, and low-energy electromagnetic backgrounds rapidly become worse. For larger angles the counting rates are too low to justify an increased detector size.

The major challenges in an asymmetry measurement of this sort are to extract the signal in the presence of a large symmetric background, and to ensure that there are no background asymmetries which can cause significant errors. Most of the backgrounds involve mistaking a decay γ from a π^0 (or other hadron) for a scattered e or directly-produced γ. The largest background is in fact from π^o electroproduction, $ep \to e\pi^o x$. One must also consider photoproduction backgrounds (arising from forward real or virtual bremsstrahlung photons) and accidentals.

In the following sections the various backgrounds and possible spurious asymmetries due to them will be described in detail, along with methods for suppressing, estimating or measuring them; and estimates of the achievable statistical precision and systematic uncertainties will be presented. We will conclude the present section with a few general remarks.

First, if one simply averages over the entire cut acceptance, the signal-to-noise ratio is only 1-2%. However, many kinematic regions have expected asymmetries of >5%, and by looking mainly in favorable regions (for example, those with a large ratio of $|T_{int}|^2$ to the background) one can substantially enhance the signal-to-noise. Second, whenever one particle can be explicitly identified as a π^o (or η) decay product, the event is no longer a background. Third, a significant spurious asymmetry can arise from a very small effect (even .3%) which affects a large background process such as π^o photo-or electroproduction. However, most such effects can be directly measured by comparing identified "e"π^o events for the two polarities, or often even from comparisons of $e^{\pm}$ inelastic scattering; these measurements can be made simultaneously with the main experiment. Finally, $e^{\pm}$ inelastic scattering asymmetries and (single-polarity) $e\pi^o$ and $e\eta$ electroproduction provide interesting auxiliary experiments in their own right, and can be measured (as will be described) by using appropriate cuts to make it highly probable that the "electron" is indeed an electron.

B. Symmetric Backgrounds

Most backgrounds are the same for e^+ and e^- beams; hence they cancel in the subtraction. However, because the backgrounds are usually more than 20 times the signal, they are the major source of statistical errors in the results of this experiment. Some of these symmetric backgrounds are:

1) $ep \rightarrow e\pi^0 X$, where the π^0 decays into two photons, one of which produces a shower which, with the electron shower, passes all cuts. The opening angle of the two photons from such a π^0 is almost always over 20 mr; so we need not worry about both photons together simulating a single shower. Apparent x and q^2 can be computed for the reaction as if the π^0 decay photon were from the 3γ process. Table 1 shows the Monte Carlo computed distribution in x and $-q^2$ for those events of this background for which both photons entered the detector, while Table 2 shows the distribution of events for which the π^0 cannot be reconstructed because one of the photons missed the detector. These tables are based on an inclusive π^0 spectrum from E88 results and assume 100 hours of 10^8 e/pulse at 180 pulses/second through a 12.5-cm LH_2 target. Comparison of Tables 1 & 2 shows that about 3/4 of this background can in principle be eliminated by reconstruction of the π^0, provided our π^0 mass resolution is adequate.

The standard deviation in measured mass for a π^0 of energy E_π decaying into two photons with opening angle θ is

$$\sigma_m = \left[6.25 \times 10^{-3}\ E_\pi \sin^2 \theta/2 + \frac{2\times10^{-6} m_\pi^2}{\sin^2\theta/2}\right]^{1/2} , \qquad (8)$$

where "6.25×10^{-3}" corresponds to an energy measurement error growing like $\sqrt{E}$ and which is 2.5% at 10 GeV, while "2×10^{-6}" corresponds to a 2 mr angular resolution. Our actual angular resolution may well be better (see Section VB). For a typical $E_\pi \sim 7$ GeV and $\theta \sim 40$ mr we get $\frac{\sigma_m}{m_\pi} \sim 8\%$ (primarily determined by the angular resolution). In E99 we were able to see a clear π^0 peak in spite of the much inferior mass resolution. However, π^0 decays for which one photon has only a few hundred MeV may be difficult to separate out because of pileup. About 1/4 of all the lower energy photons that hit the detector from this background are under 500 MeV.

Although we have not carefully considered the analogous background from η^0, this background should be much less than that from π^0, and should also be partially separable (though to a lesser degree).

2) Non-interference Bethe-Heitler and Compton events -- $ep \to e\gamma X$. In most kinematic regions these backgrounds are far smaller than that from $ep \to e\pi^0 X$ (see Tables 3 and 4).

3) Accidental coincidences. Two electrons from different events can simulate a single two-shower event which passes all cuts. Similarly, the two showers can come from an electron of one event in accidental coincidence with a photon from a π^0 decay of another event, or two photons can come from two π^0 decays in accidental coincidence. A Monte Carlo estimate of the combined backgrounds

from these processes is shown in Table 5. Only the dominant single particle sources have been included: inelastically scattered electrons and π^o's photoproduced by real or nearly real photons radiated in the target. Other sources of accidentals are expected to be much smaller than the ones included.

It is clear that some of the accidental background can be removed by explicit π^o identification, but in any case, accidentals don't contribute much of the background.

4) $\gamma + p \rightarrow 2\pi^o + X$. i.e., photoproduction of two π^o by a real or virtual photon with a photon from each π^o passing all cuts.

We have estimated the inclusive π^o decay photon spectrum from real and near real photons associated with the $e^\pm$ beam. Table 6 compares that photon spectrum with the inclusive $e^\pm$ spectrum as a function of apparent $\tilde{q}^2$. It is seen that there are somewhat more single electrons with $|\tilde{q}^2| > 2$ than there are photons. From this observation, the following reasoning leads us to conclude that the background from two-π^o photoproduction will be considerably smaller than the one from $ep \rightarrow e\pi^o X$:

Given that one π^o is produced that leads to a photon of high apparent $\tilde{q}^2$, there is a certain 4-momentum left available for the possible production of another π^o. The situation is kinematically similar to the case where the high $\tilde{q}^2$ photon is replaced by an $e^\pm$, in which case the remaining 4-momentum is that of a virtual photon, and we have already discussed the background from this similar case. For our present case, however, there is less energy available for the second π^o because a) the incoming real or near-real photon energy is less than the full electron beam energy and b) some of the energy is in the second photon of the first π^o. Thus even if we don't identify and remove obvious π^o's, we can expect this background to be less than that from $ep \to e\pi^o X$. And of course if we do exclude events for which one of the showers is from a π^o, this two-π^o process gives us two chances to identify such an event as background. We have neglected this process in our estimates of statistical errors from backgrounds, but it will be studied in runs with the $e^{\pm}$ beam replaced by a bremsstrahlung photon beam.

C. Statistical Extraction of the Signal

In most kinematic regions the signal is very small compared with the background. Yet in some kinematic regions the signal is expected to reach 5-10% of the background. It would therefore be reasonable to make additional cuts to those scaling region cuts discussed in Sections IV A and D -- cuts such that only kinematic regions with a comparatively large signal are used in the analysis. More generally, one may assign each event a weight which is zero or small where the signal is not expected to be significant compared with the background and which is large where we do anticipate a significant signal. If we use a weighting scheme that is chosen before we look at the data, the V(x) can be computed in an unbiased way by comparing the observed weighted difference between e^+ and e^- with the weighted difference per unit V(x) predicted by a Monte Carlo simulation of the experiment. The weight we intend to assign to each event is (the anticipated interference contribution)/(anticipated background) in the kinematic region where the event is detected. It can be shown that with such a weight, if the anticipated interference contributions and backgrounds turn out to be equal to the real ones and if the measurement errors are negligible, then a) the computed V(x) will have the smallest statistical errors of any conceivable weighting scheme and b) the weighted differences, which hereafter we will call "yields," from each kinematic region will have variances that are equal to the values of the yields. This relationship between yields and variances is the same as the one Poisson statistics gives. That is, so far as statistical errors are concerned, the yields computed in the above manner can be thought of as if they were raw numbers of events in a background-free measurement.

Table 7 shows a Monte Carlo computation of the expected yields (= variances of those yields) binned in x and $-q^2$. From the sum of the yields from all bins, we see that we expect an overall signal more than twenty standard deviations away from zero for the case of fractionally charged quarks. The fractional error in V(x) from a given $-q^2$, x bin is anticipated to be (value in that bin of Table 7)$^{-1/2}$. Figure 4 shows the V(x) used in the Monte Carlo calculation[9] along with the expected errors in our measurement of it (using all $-q^2$ bins combined). Fig. 2 gives this V(x) divided by $\nu W_2(x)$ (see Section II), again with the errors expected in our determination with fractionally charged quarks. The background assumed was the sum of all those symmetric backgrounds discussed earlier, except for $\gamma + p \rightarrow 2\pi^0 + X$. So long as the weights are not changed, the yields will not be systematically affected when the actual background turns out to be different from the one used in the weights. But the variances do depend on the background. For example, we did not assume any ability to decrease the background by identification of π^0's. If we can cut the background in half by such identification, or if for any reason the actual background is half the anticipated background, the statistical errors in the measurement of V(x) will be cut by a factor of $1/\sqrt{2}$.

In most of the tables we have neglected position and energy resolution. But Table 8 shows the size of the rms error in x measurement for each bin, and Table 9 does the same for the rms error in $-q^2$. We assumed a 2 mr angular standard deviation and a $\sqrt{E}$ dependence of the energy error with 2.5% at 10 GeV. It is seen that the bin size chosen is comparable with or smaller than the measurement errors everywhere except for x > .6 where the x error is large and where the lack of data would in any case cause us to have larger x bins. When the measurement errors are included in the Monte Carlo, the yields change slightly, the weighting scheme chosen is no longer exactly the one which gives the best measurement of V(x), and the variances of the measurements are no longer exactly equal to the yields, but they are only a few percent larger.

D. Scaling Checks

We use the notation of Figure 1. In order to guarantee that all photons in the interference term attach to the same parton and that the partons are free during the interaction, we must demand large values of $|q^2|$, $|\tilde{q}^2|$, $|\tilde{q}^2-q^2|$.[3] The cuts used in this proposal ($|q^2|>1$, $|\tilde{q}^2-q^2|>1$, $|\tilde{q}^2|>2$) are effectively the same as suggested in reference 3, but we would like to test their validity. In fact, testing scale invariance of this hitherto unmeasured structure function, $V(x)$, is one of the most important aims of this experiment.

The reaction is described by the four 4-vectors p, p', P, k. From these we can form 10 dot products, of which four are squares and are therefore constants characterizing the type of reaction (the masses squared). From the other six dot products we can form the following six independent Lorentz invariants.

$$
\begin{aligned}
&1)\ x = -q^2/2P\cdot(p-k-p'),\ \text{where} \\
&2)\ q^2 = (p-p'-k)^2, \\
&3)\ m^2_{e\gamma}/2 = (p'+k)^2/2 \approx p'\cdot k \\
&4)\ \Delta\tilde{q}^2 = (p-p')^2-(p-k)^2, \\
&5)\ \Delta E = k_o-p'_o = \frac{1}{M_p}\, P\cdot(k-p'), \\
&6)\ E = P\cdot p/M_p,
\end{aligned}
\qquad (9)
$$

V should be independent of all these Lorentz invariants except x. The first, second, third, and sixth variables can be measured without knowing which shower is caused by an $e^{\pm}$ and which by a photon, though the sixth variable will be held constant in this experiment (it's the beam energy). We can measure the magnitude, but not the sign, of the fourth and fifth variables.

One way of describing a violation of scaling would be to bin the yields (weighted differences as discussed in the previous section) in some variable other than x. Call that variable "z". A Monte Carlo calculation can predict the expected ratio between yields in various z bins, and scaling violation could show up as a deviation from the expected ratio. Table 10 shows the expected yields as a function of the scaling variables we can measure. This table can be used to estimate how well we can test scale invariance. If N_1 and N_2 are the anticipated yields (assuming scaling) in two regions of z, then our sensitivity to a scaling violation is the fractional statistical error in $\frac{N_1}{N_2}$, i.e., $\sqrt{\frac{1}{N_1}+\frac{1}{N_2}}$. For example, for $-q^2$ ranges $1 \le -q^2 \le 2$ and $2 \le -q^2 \le 4$, scale invariance should be tested to $\pm\sqrt{\frac{1}{323}+\frac{1}{89427}}$, or 11%.

E. Spurious Sources of Asymmetries

In most kinematic regions the signal is a small fraction of the background; so minor differences between e^+ and e^- backgrounds can be dangerous. Our weighting scheme is one way we minimize the effect of different backgrounds. Since highest weights are assigned to those events with highest signal to background, the effect of asymmetric backgrounds is suppressed. Even so, with the signal and backgrounds discussed earlier, Monte Carlo calculations show that if the background is enhanced 3.4% for one polarity beam and suppressed 3.4% for the other, the spurious asymmetry will be as large as the signal. To express the situation another way, if the background is .3% larger for one polarity than the other, the overall yield will have a systematic error of about one standard deviation. Before doing this experiment we must be convinced that background differences can be kept small and that we can correct for most of the differences that do show up.

Some of the sources of spurious asymmetries are:

1) Different quantameter calibrations for the two polarities. This was evaluated in the E-99 experiment and found to be much less than 0.1%.

2) e^+ annihilation radiation. As was discussed in the section on symmetric backgrounds, both e^+ and e^- produce backgrounds from decays of $2\pi^0$'s photoproduced by real or virtual bremsstrahlung. But e^+ contributes an additional photon beam from annihilation with e^- in the target. Because this photon spectrum is peaked near the beam energy, it could be an especially dangerous source of asymmetric background. To get a rough idea of how much asymmetry these photons contribute, we use the fact that the ratio between the annihilation and bremsstrahlung cross sections is [10]

$$\left(\frac{d\sigma_{e^+e^-\to\gamma\gamma}}{dk_o}\right)\Big/\left(\frac{d\sigma_{brems}}{dk_o}\right) = \frac{10}{\gamma}\,\frac{1}{\frac{1}{2\gamma}+(1-y)} , \qquad (10)$$

where $\gamma = E/m$ for the incoming lepton and $y = k_o/E$. We are concerned with a background that is most serious for large y. Take $\left(d\sigma_{brems}/dk_o\right)$ roughly constant; so the fractional contribution from $y > y_o$ is very crudely

$$\frac{\int_{y=y_o}^{1}\left(\frac{d\sigma_{ee\to\gamma\gamma}}{dk_o}\right)dk_o}{\int_{y_o}^{1}\left(\frac{d\sigma_{brems}}{dk_o}\right)dk_o} \approx \frac{\int_{y_o}^{1}\frac{10}{\gamma}\,\frac{1}{\frac{1}{2\gamma}+(1-y)}}{\int_{y_o}^{1}1} \approx \frac{10\log 2\gamma(1-y_o)}{\gamma(1-y_o)}$$

$\approx$ 1% for $y_o = 3/4$. $\gamma + p \rightarrow 2\pi^0 + X$ is a source of just a fraction of the background; so we see that although we may need to make a correction for this asymmetry, the correction will be a small part of the signal. Since we intend to measure backgrounds with a photon beam, we could compute this asymmetry from knowledge of the background as a function of photon energy.

3) Differences in the beam energies. Monte Carlo computations have shown that a 0.5% difference between e^+ and e^- beam energies would change the overall yield by one standard deviation. There should be no trouble getting the difference well below this value[11] (the magnetic field that determines this energy is monitored with a flip coil; so hysteresis effects are irrelevant.)

4) Differences in energy calibration. Monte Carlo studies have shown that a 0.1% systematic difference between average counter calibration for the two polarities would change the overall yield by one standard deviation. We have no way of maintaining absolute calibration to anywhere near this accuracy; but because beam line magnet currents are not changed in magnitude, the line voltages should not depend on polarity, and because the detector uses no magnets, stray fields should not cause the phototube calibration to depend on polarity. Phototube drifts can be expected typically to cause no more than a 1-2% change in gain for each tube over a few hours, and these

gain drifts should be uncorrelated between tubes, if temperatures are kept well controlled. Serious rapid drifts will be detected by our calibration system and either corrected for, or used as a reason for excluding the drifting tube from use in the analysis. A correlated systematic shift will be detectable using π° and η mass peaks. See Section VC for a further discussion of calibration techniques. If the drifts are uncorrelated, then the ~1% effect for each tube should average out to less than 0.1% for the hundreds of tubes we will actually have. Furthermore, since we anticipate reversing polarity about 100 times during this experiment, random gain drifts will tend to cancel out, even if many phototubes have correlated uncorrected drifts. This frequent polarity reversal will reduce the systematic calibration difference by another factor of 10 to as low as .01%.

From past experience with lead glass at similar angles with respect to a similar beam to the one we propose using, we know that pileup of very low energy accidental particles can cause shifts (at worst - for small angles - of the order of 50 MeV) in energy measurements. Section VB discusses several methods for minimizing the amount of pileup. These shifts will be measured by collecting energy spectra for every counter element when no high-energy particle is nearby. Although the absence of a magnet in our detector should make the pileup about equal for the two polarities, actual running intensity may have to be decreased if tests show that polarity differences in pileup could significantly affect our measurement. In a previous experiment (see Appendix) we ran at 3 carefully controlled different intensities in order to place limits on intensity-dependent effects. We anticipate doing the same in this experiment.

5) The three-photon process for which the relevant photon doesn't trigger the detector, but for which a π^0 decay photon does cause the event to pass all cuts. Because this process is the same interference term as the one we are proposing to measure, we can estimate it by the same theory, provided we make some additional assumptions.

In a previous experiment (E88) we measured the π^0 electroproduction direction and energy spectrum as a function of virtual photon 4-momentum. Here we have assumed the same behavior as a function of the available 4-momentum, even though that 4-momentum is not in the form of a virtual photon. We have also assumed* that the theory for the three-photon process applies down to $|q^2| = .4$, and we have neglected events with $|q^2|<.4$. A Monte Carlo computation then gave less than a one standard deviation shift in the yield.

The process calculated in this way may be regarded as a hard-photon radiative correction to $ep \to e\pi^0 X$ (with

*For the purposes of this particular calculation only.

the <u>detected</u> photon coming from π^o decay). More generally, one should also consider the case of softer radiated photons. In the infrared limit, one is concerned with the interference between an amplitude to emit a photon from an electron line and an amplitude to emit a photon from an external hadron line. (The divergent part is cancelled by the infrared part of the internal radiative correction involving a photon linking the same two lines.) Such corrections[11] are multiplicative, and (since the π^o itself doesn't radiate) ought to be the same for π^o electroproduction as for inelastic electron scattering. The lack of an observed asymmetry for the latter process[1] is thus an indication that such effects will not be important for the former. (The present experiment will repeat the single-particle e^+/e^- asymmetry measurements with higher precision, and extend them to higher $|\tilde{q}^2|$.) We recognize that there is a range of harder photons for which neither this argument nor the one in the preceding paragraph is strictly applicable. (Moreover, one must also allow the possibility that two-photon-exchange rates could differ between $e^{\pm}$ and $e^{\pm}\pi^o$ final states.) While there is no reason to expect a large asymmetry from these radiative corrections, we should check this empirically. The procedure to be discussed at the end of this section does this.

6) The three-photon process for which the $e^{\pm}$ doesn't trigger

the detector but for which a π^0 decay photon replaces the electron in producing a shower that satisfies all cuts. With the same approximations and assumptions as for the previous source of spurious asymmetry, a Monte Carlo computation gave an effect less than one standard deviation in size and in the opposite direction to that from the previous source of spurious asymmetries.

We will be able to measure and correct for the asymmetries of all backgrounds which involve a π^0 decay photon. We will have over a million triggers that simulate the three-photon process but which later are rejected because what seemed to be one shower is seen to be caused by two π^0 decay photons. Unless it is very near the edge of the detector (and we need not accept such events), a π^0 with enough energy to simulate a three-photon-process shower that passes all cuts will be able to decay in a way that can be reconstructed as a π^0. If these reconstructable background triggers show an asymmetry between e^+ and e^- beams, a Monte Carlo program can randomly toss the center of mass π^0 decay direction in a spherically symmetric manner, and we can then compute the asymmetry produced by those π^0 decays which cannot be reconstructed.

F. Simultaneous Measurements

While data are being collected for the three-photon process, we will also be able to trigger on deep inelastic $e^\pm$ scattering. While the photon background does not permit accurate absolute measurements, we can make sufficiently good measurements at large $|\tilde{q}^2|$ to check on our understanding of the apparatus and backgrounds.

Moreover, it is more important to extend our earlier measurement (see Appendix) of the difference between e^+ and e^- inelastic electron scattering, since the backgrounds will then cancel. If there is any π^o background asymmetry, it can be identified and subtracted in the manner discussed in Section IVE. Another possible technique for eliminating background derives from the fact that its kinematic distribution differs from that of the foreground. For a given $\tilde{q}^2 = -4EE'\sin^2\theta/2$, the background tends to have lower $p_\perp = E'\sin\theta$ than the foreground. As an example of what can be done with such a kinematic difference, Table 11 compares the $\tilde{q}^2$ distribution of $e^\pm$ with that of photons after one cuts on shower energy according to

$$E' > \frac{.8}{\theta(1-2.5\theta)} \text{ GeV.}$$

Table 6 shows the $\tilde{q}^2$ distributions before making such a cut. Any cuts we finally impose will have their effect on backgrounds checked with the help of a bremsstrahlung photon beam.

Similar techniques will allow measurements of inclusive π^o and η electroproduction, especially in the high $|\tilde{q}^2|$ region. Again, bremsstrahlung beam measurements will allow us to check our ability to distinguish $e\pi^o$ and $e\eta$ states from (photoproduced) $\pi^o\pi^o$ and $\pi^o\eta$ states; they will also allow data to be collected on inclusive π^o and η photoproduction. At the same time data will be available on any photoproduced high mass states which decay into electrons, photons, or π^o's. Similarly, inelastic

Compton scattering information will be available on the tapes.

V. APPARATUS

A. Detector

The experimental set-up consists essentially of a hydrogen target, a shower detector, and beam monitoring devices. The detector, which is of novel design, will be discussed here.

Because of the large solid angle needed, it was economically necessary for us to go to the lead and scintillator type of detector. Liquid argon is about a factor of five more expensive, and for comparable segmentation, lead glass is even more expensive than that. In fact, for the cost of the smaller pieces of lead glass (for the region near the beam) with which we were going to augment the lead glass wall, we can build this whole detector, which will cover the same solid angle but have better energy, spatial, and time resolution than would that lead glass detector. The UCSB group already has the money to build the detector. It should also be noted that this is the same shower detector which is being proposed as one of two in PEP-9.

The showers develop in lead plates which are made mechanically stiff by being laminated between aluminum sheets. The space between the Al-Pb-Al layers is filled with a mineral oil base liquid scintillator. The liquid scintillator has two important properties: it is cheap, and it has a very long light attenuation length. In order to obtain spatial resolution, the scintillator layer between the lead plates is divided into light-channel strips. Considerable flexibility in strip configuration is possible, and in this case we would have three different directions of light collection. As is shown in Fig. 5, where portions of different strip directions are displayed, there would be x, y, and θ views. The former two would primarily determine the energy and position of the shower, while the θ direction would resolve ambiguities, lessen any problems due to multiple hits in a single x or y counter, and provide a trigger signal which gives $\tilde{q}^2$ or transverse momentum directly.

Several recent developments make the counter easy and cheap to construct. One is the use of teflon-coated surfaces to form the light channels. Teflon has an index of refraction of 1.38 so that the boundary between the liquid (index about 1.5) and the teflon is a total internal reflector for light angles less than 24°. The use of teflon surfaces in hadrometers is a fairly common practice (L. R. Sulak, Proceedings of the Calorimeter Workshop, 1975, edited by M. Atac). In present detectors, 1-mil teflon film is purchased from DuPont, aluminized to improve the efficiency for wavelength shifting in the scintillator, and coated with adhesive. The film is then squeegied onto the wetted metal surface. In large quantities the total cost for the film is about $0.40 per square foot.

The only new technique in this detector is the segmenting, or subdividing of the liquid layers into light-channel strips. We are making a prototype in which we teflonize 10-mil soft aluminum foil and form this into a square corrugated shape. When sandwiched between the teflonized lead layers, this forms a light channel for each corrugation. The shaping of the aluminum foil can be done very cheaply by private industry. We are trying two approaches: applying the DuPont film before shaping the foil, and spray-teflonizing after bending (as done on teflon-coated utensils, again by private industry). Both approaches appear to cost between $1 to $2 per square foot of segmenting foil. The choice will depend upon the quality of the resulting surface.

A major problem is the guiding of the light from the ends of the light channels to the photomultiplier tubes. In our case the light from a number of parallel light channels from different depths in the counter is to be optically added and guided to the tube. Again a recent development has greatly simplified this problem. Our plan is simply to lay a wave bar (which was first suggested by Barish), an acrylic doped with wavelength shifter, over the ends of the relevant light channels, but on the air side of a transparent window. The wavelength shifter absorbs the blue light from the scintillator and reemits green light isotropically. The required area of the phototube which is glued to the end of the wave bar can be small, since Liouville's Theorem does not apply to this inelastic process. Our calculation indicates that a sufficient number of photoelectrons should be produced at the photocathode so that photoelectron statistics are not the major component determining the energy resolution of the detector. The wave bars make possible the extraction of light from the θ counters illustrated in Fig. 5.

With the low price of scintillator strips, which this liquid technique provides, and with simple large-area light collection, one can build counters with many thin lead layers and therefore improve the resolution over that normally associated with lead-scintillator counters. We plan to study the attainable resolution in a SLAC test beam in May, using the prototype now being built. If the test for some reason indicates that the liquid scintillator system will not work, a fallback position will be to use a cheap acrylic plastic scintillator, at somewhat higher cost.

B. <u>Detector Segmentation : Pileup and Resolution</u>

Several considerations (besides cost) are important in determining the depth, sampling frequency, and segmentation (both transverse and longitudinal) of the shower detector. These include energy and angular resolution, minimum sensitivity to charged pions, and keeping pileup (the ubiquitous low-energy electromagnetic background) to an acceptable level. While the design has not yet been fully optimized, this section will describe a plausible configuration.

Shower Monte Carlo calculations have been done for a lead-scintillator sandwich consisting of four samples per radiation length, with alternate samples being x and y strips. (The triggering "θ-counters" do not need as good resolution as the x and y counters; they can occur less frequently and sample between the same pairs of lead plates as some of the x and y counters.) For 8 GeV electrons, the calculated total energy resolution of a 14 radiation-length counter came to about 3% rms (consistent with

$\approx .085/\sqrt{E}$). Thus a 16 radiation-length counter ought to provide adequate resolution for both e's and γ's. This sort of resolution is reasonable, based on what others have obtained with such counters.

If a shower detector is too deep, charged hadrons which interact in the detector can start to be a significant background. (Of course, without a magnet this will largely be a symmetric background.) In a 21-GeV bremsstrahlung beam experiment (E-76) we found that the charged pion contamination to photon spectra above 7 GeV was only 2-3% for 14-radiation-length lead glass counters. From this point of view, a 14-16 radiation length detector is therefore acceptable.

With a strip width of 2", the shower Monte Carlo calculation predicts an rms position resolution of $\approx$0.5 cm. This is obtained using linear weighting by the energies in adjacent strips (which is not necessarily the optimum method) and for a detector at 240" from the target translates into < 1 mr. Note that a resolution of 2 mr was assumed in the π^o mass discussion of IVB.

For angles $\leq 9^o$, pileup considerations have led us to select a strip width of 1" rather than 2". Pileup is a problem both because of its effect on π^o mass resolution (if one photon has only $\approx$0.5 GeV), but also because it can be asymmetric between $e^{\pm}$ beams. (A correction can be made, but this becomes difficult if the pileup is very large. See Section IVE.) Based on crude measurements made during our π^o electroproduction experiment (E-88), we estimate an average extra energy of $\approx$ 40-80 MeV per 20 nsec gate for the smallest-angle strips. The effect drops rapidly with angle (probably like θ^{-4}). A radiation length of low-Z material preceding the detector can reduce the mean pile-up energy by about half.

For high energy showers, achieving the calculated energy resolution requires summing 2 or 3 adjacent 2" strips (even for normal incidence). This shower-spreading occurs mostly beyond shower maximum, whereas any pileup is concentrated in the first few radiation lengths. To avoid adding in pileup from more than one strip, one can longitudinally segment the x and y counters (at least at smaller angles), with the first ≈3 radiation lengths going to a separate phototube. Then only 1 (or occasionally 2) 1" upstream strip need be included in the energy sum. (The shower position can first be determined by using the downstream strips.) If we adopt this procedure, all the downstream strips can probably be 2" wide. This results in a total of approximately 600 phototubes for all the x and y counters. The θ counters require approximately 100 more.

The various resolution properties (aside from the effect of pileup) will be tested in a SLAC beam during the next month or two, and a firmer design settled after that time.

C. <u>Triggering and Trigger Rates</u>

The Monte Carlo yield calculations predict that in the region of interest for the three photon process the azimuthal angle difference between the e and the γ is greater than about 110°. A low-energy cut of 4.5 GeV for each particle was used in all yield computations, and was found to eliminate a negligible amount of useful data. One might therefore envision a trigger based on detector quadrants (or if necessary on octants separated by at least 90°), with the requirement that two such segments each have total energy >4.5 GeV. However, such a loose trigger gives unacceptably large background trigger rates from the smaller angles. For this reason we have included θ-counters so that a weighted sum of counter pulse heights can simulate the $|\tilde{q}^2| \geq 2$ GeV^2 cuts. Then the expected trigger rate from the dominant $e\pi^0$ electroproduction background is approximately 1 1/2 per second (at 10^8 $e^{\pm}$/pulse, 180 pps). The trigger rate for all coincidence processes should be less than double this.

For a simultaneous measurement of inelastic electron scattering, an asymmetry measurement good to 0.2% in each of four $\tilde{q}^2$ bins would require less than 10^6 single-particle triggers per polarity or an additional 3/second. (One can pre-scale the raw data rates in each $\tilde{q}^2$ bin.) Even including calibration triggers, the overall trigger rate should be no more than 5 to 10 per second.

D. Calibration

Calibration of the detector has two aspects: energy calibration of each strip with an electron beam; and gain-tracking between such runs. We propose to do the electron beam calibration by using horizontal detector motion and vertical magnetic deflection. For the former, it is natural to use the existing End Station A system of rails. Our planned target-to-detector distance is 20 feet. One reasonable plan is to position the detector on the 43-foot rails and the H_2 target 23 feet downstream of the pivot. Then an 18D72 magnet located just upstream of the pivot would be able to sweep 10 GeV $e^{\pm}$ to the vertical extremes of the detector. (Even for a magnet located at the pivot, just 40 kg-m would be needed.) If instead the 25 foot rails are used, an 18D72 just upstream of the pivot would allow calibration with 6 GeV $e^{\pm}$, which is all right provided pulser linearity measurements can be made for larger pulse heights. Precise locations will be worked out in discussion with SLAC. A minor disadvantage of the 43-foot location is that the calibration particles will not enter the detector at the same angles of incidence as target-produced particles. However, corrections can be made for this, and the effect is polarity-independent.

The calibration procedure involves putting a very low-intensity (1 particle/pulse) 10 pps $e^{\pm}$ beam into each of the $\approx$400 strips. (The number is smaller if one can be simultaneously changing both horizontal and vertical position.) This will have to be done at the start and end of the experiment and, as a check, once or more in between. (This depends on the calendar running time.) On at least one occasion, an extra set of points will be needed to measure any attenuation along the length of the counters. Each point will take about one minute to run. For the vertical (magnetic) scans, moving from point to point can be easily automated. Maximum efficiency requires that the same be done with the horizontal (cart movement) scans, although a convenient physicist-operated remote control system will be adequate. Thus the entire procedure should take no more than 1 to 1 1/2 shifts at 10 pps for each occasion it is done, plus perhaps an extra two shifts for detailed attenuation studies.

Gain-tracking can be done by several methods. One, which we've used in many (albeit smaller) experiments, is to distribute light pulses to all the counters and normalize by the light seen by two (redundant) vacuum photodiodes. In addition, however, one can utilize actual data events to do corrections (probably offline). For example, a cross-check of x vs y vs θ counters and of upstream vs downstream longitudinal segments can be analyzed to pick out gain changes. Another method which others have used successfully[13] is to use π^0 and η mass peaks (assigning gain corrections, if needed, to the counter having the higher-energy photon, and iterating). Probably both pulser and data methods will be used. The light pulser method lends itself easily to measuring counter-tube-ADC response curves; moreover, it is easy to get online feedback from it, as will be necessary if any gain change is significant enough to affect triggering thresholds, or if a counter malfunctions.

Two additional precautions will be taken to minimize any effect gain changes might have on the asymmetry measurement. First, we will choose phototubes which we have found to be relatively stable over long time periods. (For example, RCA 6342A's meet this requirement.) Second, we will switch beam polarities as frequently as possible. If the changeover takes 5 minutes,[11] one can reasonably expect to switch at least every hour.

E. Data Collection and Logging

For every event, we will digitize the pulse area for each counter, and the timing for at least all downstream segments. With our estimated trigger rates, writing everything on tape would generate one to two 800 bpi tapes per hour. Some modest preprocessing and packing can reduce this by a factor of two to four, which should be a quite manageable level.

VI. REQUIREMENTS FROM SLAC

A. End Station A

1) Cart: A cart capable of supporting the 11-ton detector and moving (with remote control) on ESA rails. See Section VD for a discussion of possible locations.

2) Target: A 5" liquid hydrogen target located approximately 20 feet upstream of the detector. It should be possible to move the target assembly horizontally out of the beam to avoid interference with vertically pitched calibration electrons.

3) Calibration Magnet: An 18D72 for vertical steering in calibration runs, to be located near the ESA pivot (or at any mutually agreed-upon location). Interlocking of some sort may be needed to ensure that the magnet is not used except with very low intensity beams.

4) Quantameter Beam Dump and Shielding: The only shielding needed will be to protect the detector from the beam dump. If this is located far back, the quantity of shielding will not be large. We will probably also require vacuum for most of the distance. (Vacuum pipe upstream of the detector should be removeable for calibration.)

5) Cabling: Our present plan is to form energy sums for triggering in the End Station, so that we would require only one complete set (about 700-800) of Foam 8 (or equivalent) cables, plus high voltage cables or remote control. The small number of triggering cables should be run by as short a route as possible.

6) Computer: We may require the use of one of the ESA computers as part of our overall system. The details are still to be worked out.

Note: We have implicitly assumed the use of End Station A because past discussions at SLAC indicated that this would be most convenient for SLAC. (It certainly minimizes shielding costs, and many of the beam monitoring facilities needed exist there.) However, the experiment could be installed elsewhere, if there are reasons to do so.

B. Beam Requirements

1) 20 GeV e^+/e^- produced from the same source, allowing for reliable operation at intensities of at least 10^8 e/pulse. The cost of the new source required was previously estimated at $60K. (The existing source would provide only 13.5 GeV. The increased energy makes available a larger scaling region and folds the events into the detector more efficiently. At 13.5 GeV it would take about three times as long to get the same statistics as at 20 GeV, and in addition we would lose the lowest x bin and effectively the highest $|q^2|$ bin. For the scaling check at $3 \leq |q^2| \leq 5$ $(\mathrm{GeV/c})^2$, about 10 times the running time would be required for the same statistics.)

2) Rapid polarity switching: We have been told[11] that a 5-minute changeover between e^- and e^+ running is possible. This is important in order to reduce the systematic errors contributed by any time-dependent effects.

3) Beam positioning: We require precise monitoring and ease of steering; automatic steering upon setting up a given polarity would be best. Existing ESA facilities will perform these tasks.

4) Availability of low intensity beam: For purposes of calibration, it should be possible to reduce the beam intensity to the level of one particle per pulse.

5) Availability of Bremsstrahlung photon beam: To be made from the e^+/e^- beam in a radiator of the order of .01 radiation lengths thick.

C. Running Time and Schedule

The yield calculations have been done for an efficient 100 hours (at 180 pps) per polarity, for 10^8 $e^{\pm}$/pulse. Because of inefficiencies, and especially because of the probable need to do some of the running (as a check) at a lower intensity, we believe about 200 hours per polarity will be needed. An additional 100 hours will be used for photon beam running and various checks. We are therefore requesting a total of 500 hours at 180 pps.

We will additionally require about 250 hours at 10-20 pps for initial check-out and calibration, plus an additional 50 to 100 such hours during the course of the experiment (at times to be scheduled) for calibration repeats and other tests; the need for these will be proportional to the calendar time required to obtain our 3.24×10^8 "data" pulses.

The detector, the money for which must be spent by October 1, 1977, can be built by about Feb., 1978. At least two months will be required to check out its operation with the laser light pulser. The earliest installation time at SLAC would be the Spring of 1978, or whenever after that there is a convenient shutdown.

References

1. D. L. Fancher, D. O. Caldwell, J. P. Cumalat, A. M. Eisner, T. P. McPharlin, R. J. Morrison, F. V. Murphy, and S. J. Yellin, Phys. Rev. Letters 37, 1323 (1976).
2. D. L. Fancher, D. O. Caldwell, J. P. Cumalat, A. M. Eisner, T. P. McPharlin, R. J. Morrison, F. J. Murphy, and S. J. Yellin, Phys. Rev. Letters 38, 800 (1977).
3. S. J. Brodsky, J. F. Gunion, and R. L. Jaffe, Phys. Rev. D6, 2487 (1972).
4. A. M. Eisner, D. O. Caldwell, J. P. Cumalat, B. N. Kendall, T. P. McPharlin, R. J. Morrison, and F. V. Murphy, Phys. Rev. Letters 33, 865 (1974).
5. D. O. Caldwell, A. M. Eisner, V. B. Elings, B. N. Kendall, T. P. McPharlin, R. J. Morrison, F. V. Murphy, and B. W. Worster, Phys. Rev. Letters 33, 868 (1974).
6. M. S. Chanowitz, private communication (but to be published); some of the ideas about color detection below color threshold appear in M. S. Chanowitz, LBL-5312 (1976).
7. J. Pati, private communication.
8. R. J. Morrison, submitted to Nuclear Physics (1976).
9. R. Blankenbecler, et al. SLAC PUB 1531 (1975).
10. Y.-S. Tsai, Reviews of Modern Physics 46, 815 (1974).
11. Roger Miller, private communications.
12. See, for example, Y.-S. Tsai, Phys. Rev. 122, 1898 (1961); A. Bartl and P. Urban, Acta Phys. Austriaca 24, 139 (1966); etc.
13. University of Toronto experiment at Argonne (Jim Prentice, private communication).

Tables

The following tables are discussed in section IV. The coordinates printed represent the lower edges of bins. "Backgrounds" and "number of events" are Monte Carlo estimates based on 100 hours of $10^8 e^{\pm}$/pulse, 180 pulses per second through a 12.5 cm LH_2 target.

Table 1. Background from π^o's which produce one triggering photon and one photon seen elsewhere in the detector.

Table 2. Background from π^o's when only one photon enters the detector.

Table 3. Total number of Compton events at each polarity.

Table 4. Total number of Bethe Heitler events at each polarity.

Table 5. Total number of accidentals per $x - |q^2|$ bin at each polarity.

Table 6. Total number of electrons and photons as a function of $|\tilde{q}^2|$.

Table 7. Number of (standard deviations squared) of the measurement. X and $|-q^2|$ values are for lower edges of bins.

Table 8. Error in x as a function of x, $-q^2$.

Table 9. Error in q-squared as a function of x, $-q^2$.

Table 10. Yields as a function of "z" = various scaling variables (see section IV D).

Table 11. Total number of electrons and photons as a function of $|\tilde{q}^2|$ with the requirement that $E' > \frac{.8}{\theta(1-2.5\theta)}$.

BACKGROUND FROM PI-0 S WHICH PRODUCE ONE TRIGGERING PHOTON AND ONE PHOTON SEEN ELSEWHERE IN THE DETECTOR

X / -0 SQUARED	0.0	.1	.2	.3	.4	.5	.6	.7	.8	.9	TOTALS
0.0	0.000	0.000	0.000	0.000	0.000	0.000	0.000	0.000	0.000	0.000	0.000
1.0	0.000	39120.956	96971.377	45405.894	23092.852	6519.741	484.023	946.893	[illegible]	5.972	212547.159
2.0	0.000	498.323	28471.559	24372.251	17825.563	11254.682	2485.581	109.831	51.534	74.415	85643.789
3.0	0.000	0.000	4473.750	13116.468	13304.229	4119.112	3380.457	41.274	137.498	19.072	38590.872
4.0	0.000	0.000	0.000	2311.264	3673.747	1839.489	1251.785	1252.789	327.243	0.000	10706.319
5.0	0.000	0.000	0.000	110.406	1077.500	1295.549	995.629	250.460	28.228	9.471	3767.243
6.0	0.000	0.000	0.000	0.000	34.728	133.163	104.569	68.867	66.689	0.000	409.005
7.0	0.000	0.000	0.000	0.000	0.000	.133	4.559	10.592	14.77[illegible]	0.000	34.045
8.0	0.000	0.000	0.000	0.000	0.000	.366	0.000	0.000	0.000	0.000	.366
9.0	0.000	0.000	0.000	0.000	0.000	0.000	0.000	0.000	0.000	0.000	0.000
TOTALS:	0.000	39619.180	129917.296	85316.284	59808.613	25210.235	8706.593	2680.746	619.955	108.931	351637.438

Table 1

BACKGROUND FROM PI-0 S WHEN ONLY ONE PHOTON ENTERS THE DETECTOR

X / -0 SQUARED	0.0	.1	.2	.3	.4	.5	.6	.7	.8	.9	TOTALS
0.0	0.000	0.000	0.000	0.000	0.000	0.000	0.000	0.000	0.000	0.000	0.000
1.0	0.000	13159.994	22040.033	8838.617	6766.522	4904.374	4570.929	159.455	0.010	155.099	60595.159
2.0	0.000	400.394	5793.973	15221.512	6134.903	3478.303	1474.349	232.220	22.416	33.082	32792.157
3.0	0.000	0.000	939.477	2567.122	1762.712	2309.75[illegible]	286.549	27.449	0.000	11.904	7905.267
4.0	0.000	0.000	0.000	666.390	3459.185	3816.429	598.417	154.261	95.553	0.000	8790.676
5.0	0.000	0.000	0.000	51.741	410.477	199.122	459.523	172.933	106.374	0.000	1399.456
6.0	0.000	0.000	0.000	0.000	6.548	30.188	1.394	6.710	24.346	0.000	68.513
7.0	0.000	0.000	0.000	0.000	0.000	1.793	.036	0.000	44.171	0.000	46.359
8.0	0.000	0.000	0.000	0.000	0.000	0.000	0.000	.022	.177	6.309	6.539
9.0	0.000	0.000	0.000	0.000	0.000	0.000	0.000	0.000	.001	0.000	.001
TOTALS:	0.000	13560.587	28773.653	27345.138	18540.347	14740.815	7391.197	752.490	293.141	206.394	111104.107

Table 2

TOTAL NUMBER OF COMPTON EVENTS AT EACH POLARITY

X / -0 SQUARED	0.0	.1	.2	.3	.4	.5	.6	.7	.8	.9	TOTALS
0.0	0.000	0.000	0.000	0.000	0.000	0.000	0.000	0.000	0.000	0.000	0.000
1.0	0.000	1287.317	2239.233	1307.983	597.755	242.408	49.730	14.579	1.791	.056	5741.569
2.0	0.000	17.17[illegible]	544.374	603.593	408.244	104.251	57.038	7.848	1.606	.095	1744.943
3.0	0.000	0.000	41.034	175.903	115.995	50.531	15.119	3.332	.349	.058	402.515
4.0	[illegible]	[illegible]	1.305	31.551	37.913	24.755	11.025	.081	.215	.009	107.753
5.0	0.000	0.000	0.000	.435	11.525	10.636	5.770	2.217	.199	.004	30.659
6.0	0.000	0.000	0.000	0.000	.545	1.256	.179	.082	.023	.004	2.039
7.0	0.000	0.000	0.000	0.000	0.000	0.000	0.000	.061	0.000	0.000	.061
8.0	0.000	0.000	0.000	0.000	0.000	0.000	0.000	0.000	0.000	0.000	0.000
9.0	0.000	0.000	0.000	0.000	0.000	0.000	0.000	0.000	0.000	0.000	0.000
TOTALS:	0.000	1305.5[illegible]	2825.312	2119.371	1171.978	433.836	138.930	29.702	4.042	.226	8029.628

Table 3

TOTAL NUMBER OF BETHE HEITLER EVENTS AT EACH POLARITY

-Q SQUARED \ X	0.0	.1	.2	.3	.4	.5	.6	.7	.8	.9	TOTALS
0.0	0.000	0.000	0.000	0.000	0.000	0.000	0.000	0.000	0.000	0.000	0.000
1.0	0.000	953.633	2848.035	4397.167	4593.584	2517.899	1574.561	499.321	106.559	4.005	17584.803
2.0	0.000	10.401	339.455	700.143	801.199	434.771	336.702	100.165	20.977	2.202	2746.019
3.0	0.000	0.000	25.555	150.887	142.772	106.296	57.503	25.667	3.575	.584	513.004
4.0	0.000	0.000	.335	23.472	35.119	31.989	23.879	5.125	1.491	.070	121.330
5.0	0.000	0.000	0.000	.383	8.451	11.652	8.031	4.195	.344	.022	33.179
6.0	0.000	0.000	0.000	0.000	.575	1.993	.379	.292	.063	.025	3.333
7.0	0.000	0.000	0.000	0.000	0.000	0.000	0.000	.162	0.000	0.000	.162
8.0	0.000	0.000	0.000	0.000	0.000	0.000	0.000	0.000	0.000	0.000	0.030
9.0	0.000	0.000	0.000	0.000	0.000	0.000	0.000	0.000	0.000	0.000	0.000
TOTALS:	0.000	964.034	3213.931	5272.078	5581.660	3204.604	2001.120	625.127	133.050	6.907	21002.430

Table 4

TOTAL NUMBER OF ACCIDENTALS PER X -Q SQUARED BIN AT EACH POLARITY

-Q SQUARED \ X	0.0	.1	.2	.3	.4	.5	.6	.7	.8	.9	TOTALS
0.0	0.000	0.000	0.000	0.000	0.000	0.000	0.000	0.000	0.000	0.000	0.000
1.0	0.000	1137.852	1154.914	1186.090	509.318	522.625	407.035	172.737	51.146	34.001	5166.918
2.0	0.000	18.973	285.433	263.541	177.170	122.764	96.840	47.757	55.451	45.326	1113.315
3.0	0.000	0.000	27.473	70.470	52.255	26.921	17.717	13.757	11.213	25.446	245.513
4.0	0.000	0.000	1.235	12.634	11.446	8.491	9.658	4.132	2.033	1.455	52.116
5.0	0.000	0.000	0.000	.285	2.870	3.031	3.131	1.733	.323	.573	12.336
6.0	0.000	0.000	0.000	0.000	.221	.683	.171	.221	.191	.436	1.433
7.0	0.000	0.000	0.000	0.000	0.000	0.000	0.000	.123	0.000	0.000	.129
8.0	0.000	0.000	0.000	0.000	0.000	0.000	0.000	0.000	0.000	0.000	0.000
9.0	0.000	0.000	0.000	0.000	0.000	0.000	0.000	0.000	0.000	0.000	0.000
TOTALS:	0.000	1156.824	1469.151	1533.031	744.579	684.515	534.654	240.074	121.253	107.638	6591.749

Table 5

Table 6

lower edge of $|\tilde{q}^2|$ bin (GeV^2)	Electrons	Photons
0	0.	0.
1	0.	0.
2	.1639E+08	.2496E+08
3	.1742E+08	.7555E+07
4	.9577E+07	.2696E+07
5	.5588E+07	.1173E+07
6	.3103E+07	.4572E+06
7	.1775E+07	.9280E+05
8	.9296E+06	.2052E+05
9	.9205E+06	.7016E+04

Total number of electrons and photons as a function of $|\tilde{q}^2|$

NUMBER OF (STANDARD DEVIATIONS SQUARED) OF THE MEASUREMENT. X AND (-Q SQUARED) VALUES ARE FOR LOWER EDGES OF BINS.

-Q SQUARED \ X	0.0	.1	.2	.3	.4	.5	.6	.7	.8	.9	TOTALS
0.0	0.000	0.000	0.000	0.000	0.000	0.000	0.000	0.000	0.[illegible]	.[illegible]	0.00[illegible]
1.0	0.[illegible]	46.080	26.[illegible]	84.125	52.034	32.[illegible]	7.312	2.111	.1[illegible]	.002	323.[illegible]
2.0	0.000	.368	15.257	30.165	24.371	12.303	4.449	1.313	.171	.004	89.101
3.0	0.000	0.000	1.193	9.135	7.399	4.901	3.002	1.053	.157	.004	36.649
4.0	0.000	0.000	.038	1.518	3.403	3.193	2.610	.519	.1[illegible]4	.001	11.347
5.0	0.[illegible]	[illegible]	0.000	.[illegible]	.944	2.[illegible]	1.53[illegible]	.229	.0[illegible]5	.001	5.[illegible]7
6.0	0.000	0.000	0.000	0.000	.120	1.106	.175	.175	.017	.00[illegible]	1.5[illegible]6
7.0	0.000	0.000	0.000	0.000	0.000	0.000	0.000	.131	0.000	0.000	.131
8.0	0.000	0.000	0.000	0.000	0.000	0.000	0.000	0.000	0.000	0.000	0.000
9.0	0.000	0.000	0.000	0.000	0.000	0.0[illegible]	0.00[illegible]	0.[illegible]	0.[illegible]	.00[illegible]	0.0[illegible]
TOTALS:	0.[illegible]	47.[illegible]48	113.1[illegible]2	126.394	88.940	55.961	19.627	6.[illegible]70	.304	.015	457.735

Table 7

ERROR IN X AS A FUNCTION OF X, Q-SQUARED

-Q SQUARED \ X	0.0	.1	.2	.3	.4	.5	.6	.7	.8	.9
0.0	0.000	0.000	0.000	0.000	0.000	0.000	0.000	0.000	0.000	0.000
1.0	0.000	.031	.041	.072	.105	.119	.145	.194	.295	.2[illegible]
2.0	0.000	.022	.032	.044	.060	.076	.015	.17[illegible]	.13[illegible]	.1[illegible]
3.0	0.000	0.000	.027	.035	.047	.05[illegible]	.05[illegible]	.087	.1[illegible]	.0[illegible]
4.0	0.000	0.0[illegible]	.025	.031	.037	.04[illegible]	.036	.057	.077	.082
5.0	0.000	0.000	0.000	.024	.035	.044	.0[illegible]0	.056	.047	.080
6.0	0.000	0.000	0.000	0.000	.033	.037	.0[illegible]9	.043	.061	.163
7.0	0.000	0.000	0.000	0.000	0.000	0.000	0.000	.042	0.000	0.000
8.0	0.000	0.0[illegible]	0.00[illegible]	0.0[illegible]	0.000	0.0[illegible]	0.01[illegible]	0.00[illegible]	0.000	0.000
9.0	0.000	0.000	0.000	0.000	0.000	0.000	0.000	0.000	0.000	0.000

Table 8

ERROR IN Q-SQUARED AS A FUNCTION OF X, Q-SQUARED

-Q SQUARED \ X	0.0	.1	.2	.3	.4	.5	.6	.7	.8	.9
0.0	0.000	0.000	0.000	0.000	0.000	0.000	0.000	0.000	0.000	0.000
1.0	0.000	.268	.334	.4[illegible]5	.472	.424	.43[illegible]	.44[illegible]	.632	.6[illegible]
2.0	0.000	.265	.352	.390	.434	.433	.475	.532	.443	.48[illegible]
3.0	0.000	0.000	.404	.440	.490	.449	.497	.52[illegible]	.436	.493
4.0	0.000	0.000	.415	.483	.503	.530	.541	.523	.5[illegible]2	.48[illegible]
5.0	0.000	0.000	0.000	.4[illegible]1	.565	.584	.579	.558	.560	.664
6.0	0.000	0.000	0.000	0.000	.57[illegible]	.577	.676	.531	.66[illegible]	.5[illegible]
7.0	0.000	0.000	0.000	0.000	0.000	0.000	0.000	.532	0.000	0.000
8.0	0.000	0.000	0.000	0.000	0.000	0.000	0.000	0.000	0.000	0.000
9.0	0.000	0.000	0.000	0.000	0.000	0.00[illegible]	0.000	0.000	0.000	0.000

Table 9

Table 10

lower edge of "z" bin	YIELD			
z = →	$-q^2$ $(GeV/c)^2$	$m_{e\gamma}^2/2$ GeV^2	$\lvert\Delta\tilde{q}^2\rvert$ $(GeV/c)^2$	$\lvert\Delta E\rvert$ GeV
0	0	0	239	104
1	323	13	128	75
2	89	155	50	73
3	27	159	33	65
4	11	81	6	39
5	6	34	1	43
6	2	13	0	28
7	0	3	0	22
8	0	0	0	9
9	0	0	0	0

Yields as a function of "z" = various scaling variables (see section IV D).

Table 11

lower edge of $\lvert \tilde{q}^2 \rvert$ bin (GeV^2)	Electrons	Photons
0	0.	0.
1	0.	0.
2	.5239E+07	.2108E+06
3	.1314E+08	.2290E+06
4	.7419E+07	.9824E+05
5	.4192E+07	.4334E+05
6	.2254E+07	.1744E+05
7	.1292E+07	.7334E+04
8	.6925E+06	.2860E+04
9	.7267E+06	.2067E+04

Total number of electrons and photons as a function of $\lvert \tilde{q}^2 \rvert$ with the requirement that $E' > \frac{.8}{\Theta(1-2.5\Theta)}$

FIGURE CAPTIONS

Fig. 1. Diagrams for the reaction $e^{\pm} + p \rightarrow e^{\pm} + p + \gamma$ + anything.

Fig. 2. Ratios $R(x) = V(x)/\nu W_2(x)$ for various assumed forms of $V(x)$. See text, sections II and IVC, for further explanation.

Fig. 3. Schematic experimental lay-out for the previous experiment (E-99).

Fig. 4. The assumed $V(x)$, based on electron scattering results, which is used in the Monte Carlo calculations. The errors shown are the statistical determination of $V(x)$ which would result from 100 hours of full efficiency running on each polarity in the proposed experiment.

Fig. 5. Above is an overall schematic of the detector as viewed along the beam line. The sensitive region (defined by the lead) lies between the two octagons in the diagram. In order to get the light out for both x and y channels, the region containing scintillator and channels extends outward to the dotted lines. The entire detector is divided into four identical tanks; each is bounded on the inside by two edges of the inner octagon and is bounded on the outside by two half-edges of the outermost square (dotted lines). The θ wave bars are placed between pairs of tanks.

Also shown on the upper part of the diagram are some of the x channels (horizontal), y channels (vertical), and θ channels (azimuthal).

Below is a possible arrangement of the channels showing x, y and θ layers.

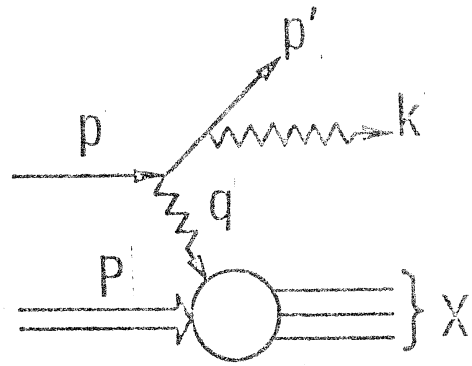

(a) Bethe-Heitler

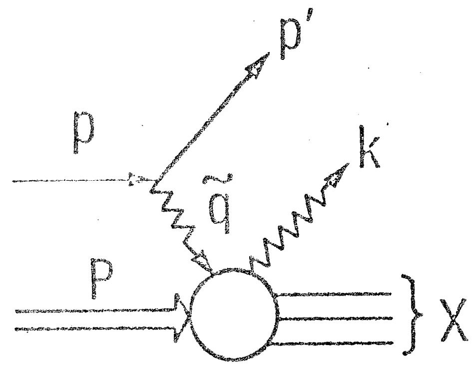

(b) Compton

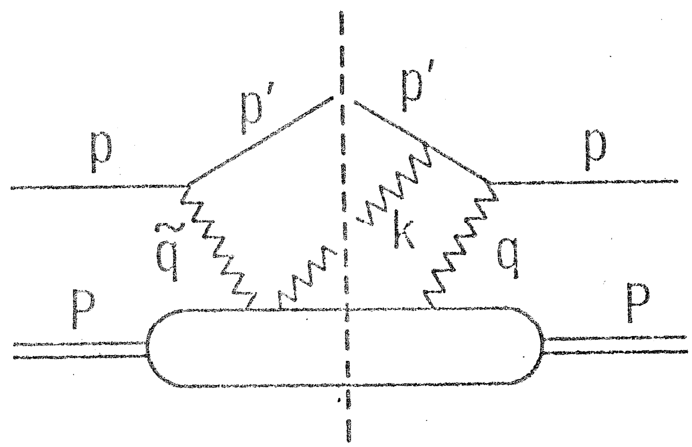

(c) Compton-Bethe-Heitler Interference

Fig. 1

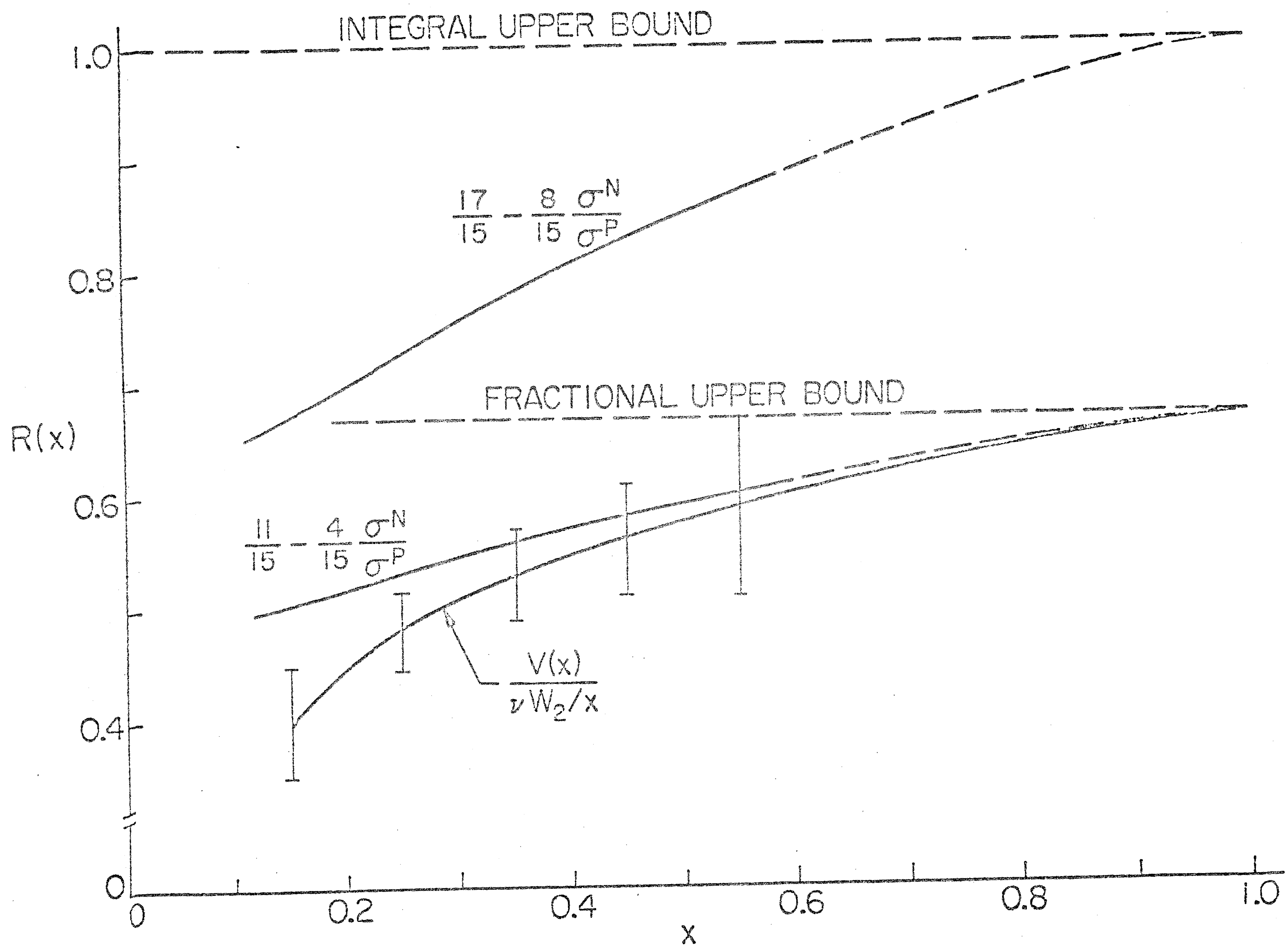

INTEGRAL UPPER BOUND
FRACTIONAL UPPER BOUND
$\frac{17}{15} - \frac{8}{15}\frac{\sigma^N}{\sigma^P}$
$\frac{11}{15} - \frac{4}{15}\frac{\sigma^N}{\sigma^P}$
$\frac{V(x)}{\nu W_2/x}$
R(x)
x
1.0
0.8
0.6
0.4
0
0.2

Fig. 2

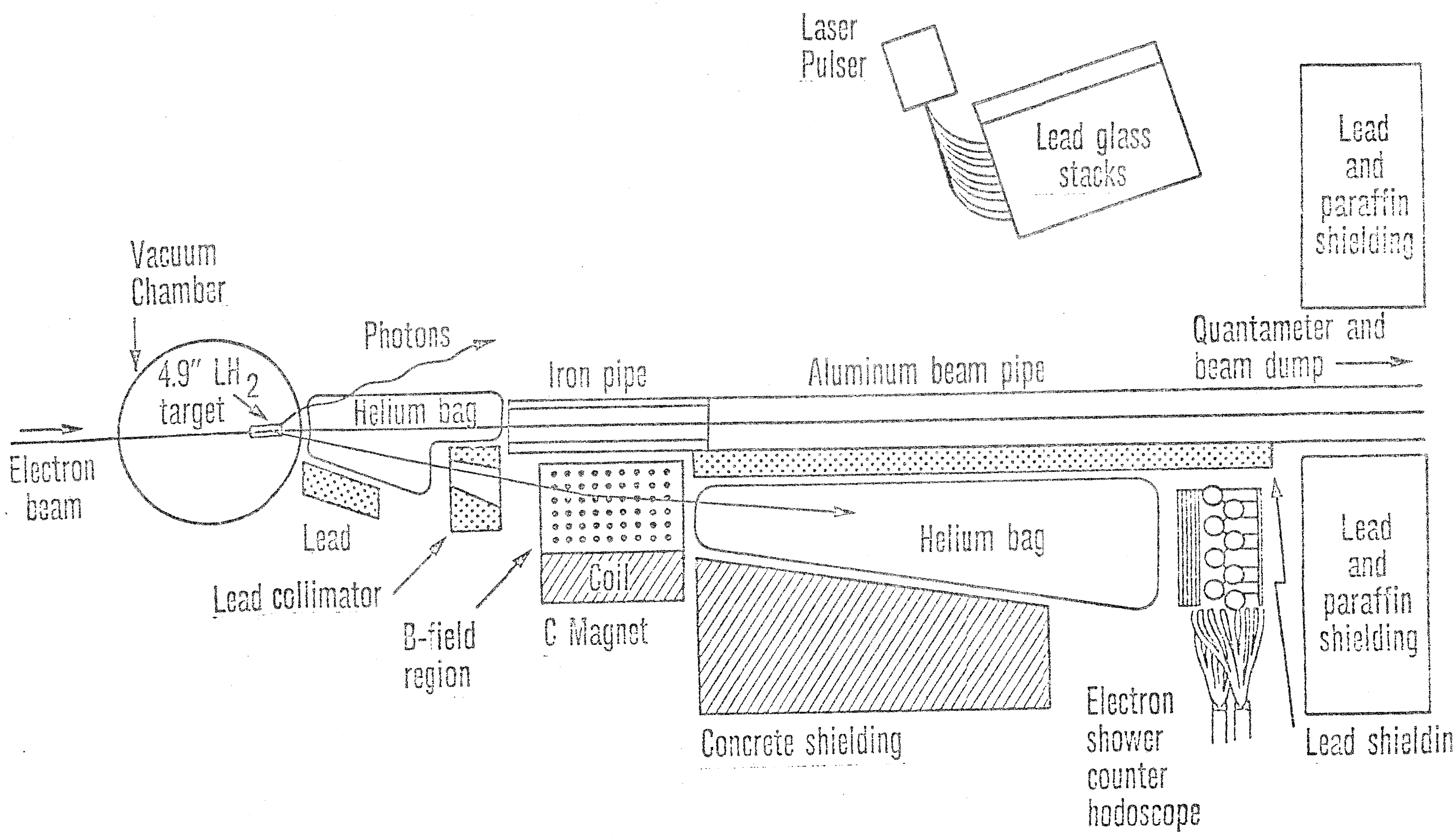
Laser
Pulser
Lead glass
stacks
Lead
and
paraffin
shielding
Vacuum
Chamber
Photons
4.9" LH2
target
Iron pipe
Aluminum beam pipe
Quantameter and
beam dump
Helium bag
Electron
beam
Lead
Lead collimator
B-field
region
Coil
C Magnet
Helium bag
Lead
and
paraffin
shielding
Concrete shielding
Electron
shower
counter
hodoscope
Lead shieldin

Fig. 3

Fig. 4

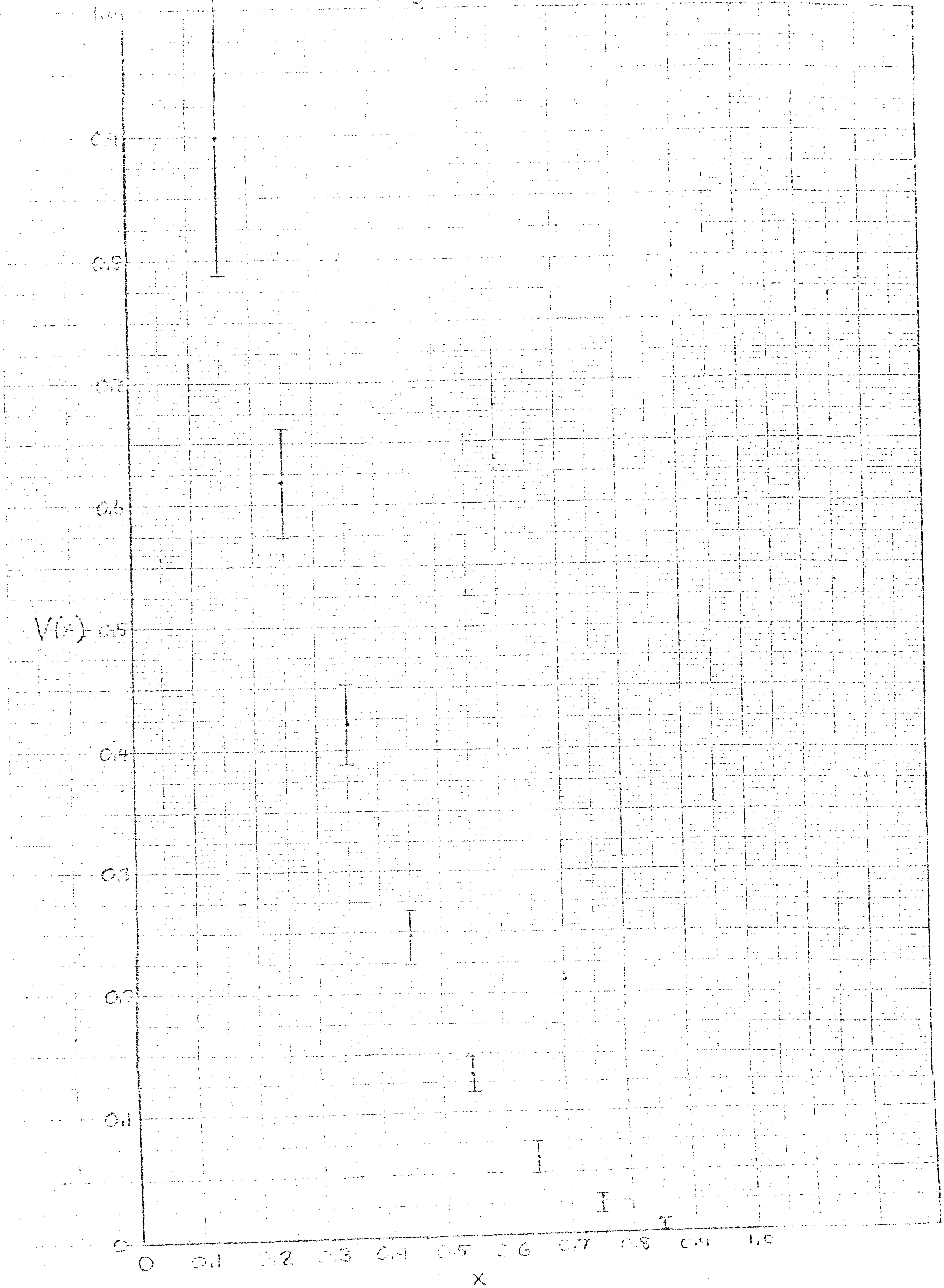

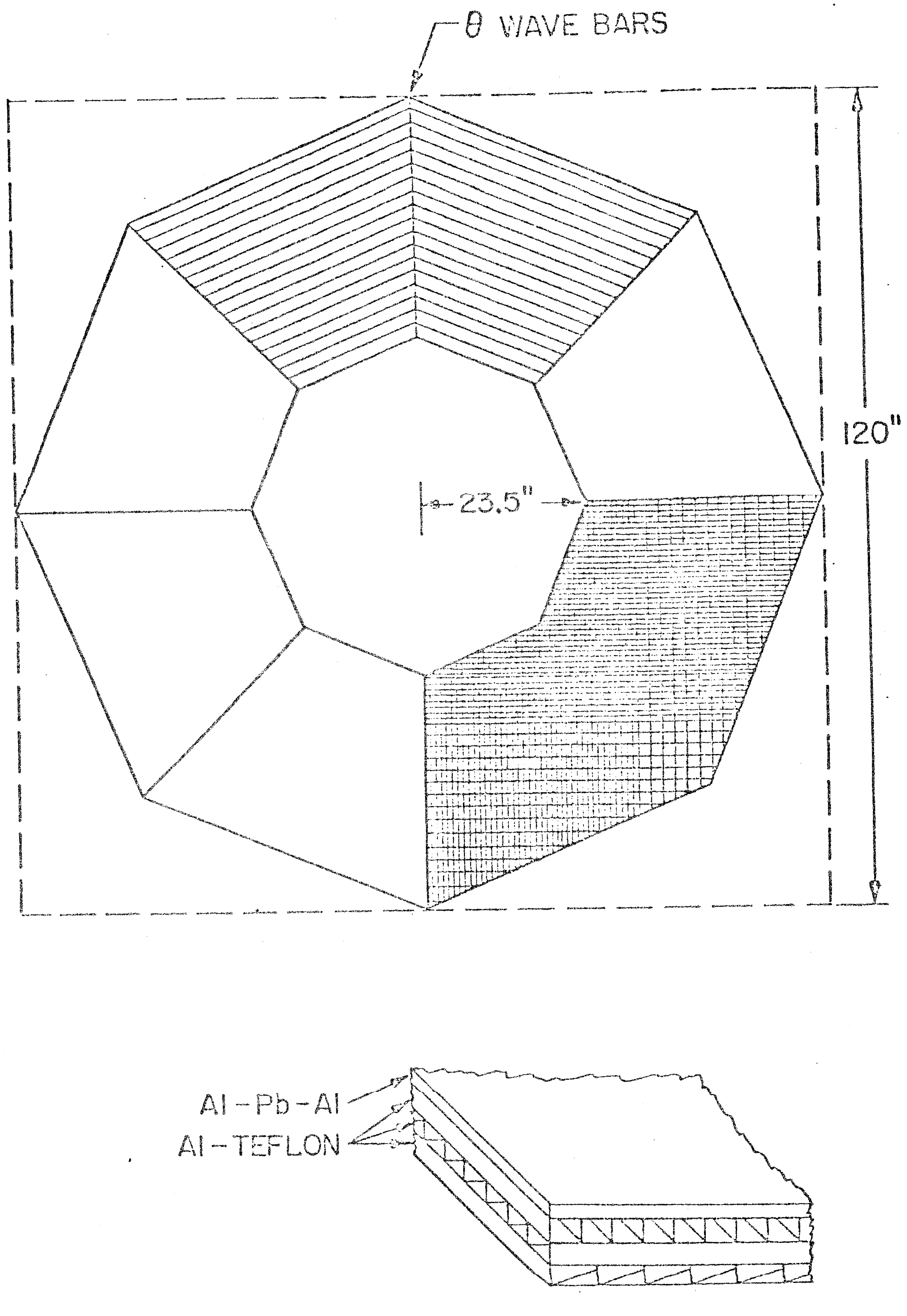

Fig. 5

APPENDIX

Precision Comparison of Inelastic Electron and Positron Scattering from Hydrogen*

D. L. Fancher, D. O. Caldwell, J. P. Cumalat, A. M. Eisner, T. P. McPharlin, R. J. Morrison, F. V. Murphy,† and S. J. Yellin
Department of Physics, University of California, Santa Barbara, California 93106
(Received 7 September 1976)

Using 13.5-GeV beams at Stanford Linear Accelerator Center, we have compared electron and positron inelastic scattering over the range $1.2 < |q^2| < 3.3$ (GeV/c)^2, $2 < \nu < 9.5$ GeV for the four-momentum and energy transfers, respectively. We find the ratio of the cross sections to be $e^+/e^- = 1.0027 \pm 0.0035$ (including statistical and systematic effects), with no significant dependence on q^2 or ν. This result has appreciably smaller errors than previous attempts to find two-photon-exchange effects in electron or muon scattering.

Numerous experiments have been performed seeking a difference between lepton and antilepton elastic[1] or inelastic[2] scattering from protons. Such a difference could occur as a result of the interference of one-photon and two-photon exchanges and might be expected to appear at about the 1% ($\sim \alpha$) level. Intermediate-state resonances or parton effects[3] could enhance this, or a type of direct lepton-hadron interaction[4] could also give a significant e^+-e^- difference. While this difference measurement could then be a potentially sensitive probe of the lepton-hadron interaction, it is certainly important for knowing the validity of the one-photon-exchange approximation, on which the whole analysis of lepton-nucleon scattering is based. We have increased considerably the accuracy to which e^+ and e^- scattering have been compared, finding no evidence for any difference to a level of about $\frac{1}{3}$%, integrated over our kinematic range of $1.2 < |q^2| < 3.3$ (GeV/c)^2 and $2 < \nu < 9.5$ GeV for the photon mass and energy, respectively.

It is obviously important in achieving such a result to make the e^+ and e^- beams as much alike as possible. Both the positrons and the electrons were produced by the electron beam in a radiator one third of the way down the Stanford Linear Accelerator Center (SLAC) linac and accelerated to 13.5 GeV in the remaining two thirds of the accelerator. Slits limited the maximum momentum spread of the beam to < 0.4%, and the position of the approximately 4-mm × 2-mm beam at the target was set to about 0.5 mm. This random setting uncertainty, which will be discussed among the systematic errors, fixed the beam angle to 0.1 mrad. Interleaved e^+ and e^- data were collected in equal amounts at three beam intensities (3×10^7, 5×10^7, and 7×10^7 e's/pulse) and no rate dependence was found even in the cross sections, making the effect on the e^+/e^- ratio completely negligible. The net beam flux was determined with a secondary-emission quantameter.

The beam interacted in a 12.5-cm liquid hydrogen target, and the scattered positrons or electrons were detected in a large-acceptance (± 5 GeV/c and 2.1 msr) spectrometer, which was set at a mean scattering angle of 8°. Particles emerging from the target passed through a magnetic field (and, for a sample of trajectories, then through thin hodoscoped scintillators at the magnet exit) and finally into a hodoscoped lead-scintillator shower detector. The shower counter was moved on rails into the main beam for energy calibrations, and it was also remotely moved vertically and horizontally in the beam to map out the detector's response.

From data on the electron's energy and position in the hodoscoped shower detector, the initial direction of the scattered $e^{\pm}$ was determined by tracing its trajectory back through the magnet to the small target. As a check on pion contamination, the momentum could be determined independently for those particles which went through the hodoscope at the exit to the magnet. Pions were detected in the shower detector with an average efficiency of only ≈5%,[5] because a minimum energy deposition of 4 GeV was required for a trigger (although all accompanying particles yielding more than 1 GeV were recorded on tape). This pion contamination, which was consistent with predicted values,[5] was measured in two other ways, and the three measurements also agreed with each other. First, the polarity of the spectrometer magnet was reversed with respect to the beam magnets. Production of a particular sign of pion should be independent of the sign of the incident beam, so this magnet reversal gave directly effective average contaminations of $\pi^-/e^- = 1.7\%$ and $\pi^+/e^+ = 3.3\%$. Second, with normal fields, sufficient lead was placed in front of the shower detectors to attenuate the electrons strongly, but to pass a known large fraction of the pions, giving corrections which agreed within their 5% error with those from the first method.

An overall check on the difference experiment was provided by a comparison of the electron yield as a function of scattered electron energy or angle with SLAC spectrometer measurements[6] of the e^- deep inelastic scattering. The fit to the SLAC results, with appropriate radiative corrections for our apparatus, was used in a Monte Carlo calculation to compare with our data. This check is a sensitive test of our acceptance calculations, energy calibrations, detection efficiency, backgrounds, and many other aspects of the experiment, almost all of which would still not affect the e^+-e^- difference, even if they did not come out correctly. However, the curves dis-

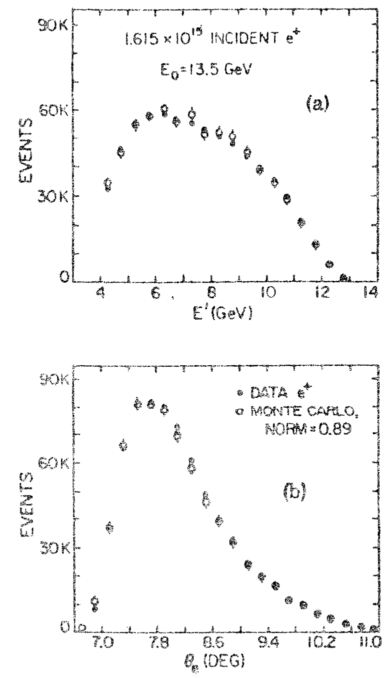

FIG. 1. Comparison of the observed electron yields, as a function of (a) scattered electron energy or (b) angle, with yields calculated by Monte Carlo, using SLAC spectrometer cross sections for inelastic scattering.

played in Fig. 1 show excellent agreement in shape for both angle and energy, which gives further confidence in the results. The Monte Carlo curves have been lowered in absolute normalization by 11% to match the data, a change which is within the error arising from the SLAC cross sections (6%, plus an additional 3% for radiative correction uncertainties) and our absolute-value errors (quantameter calibration, 5%; radiative corrections, 3%; acceptance, 2%; target length and density, 2%).

To give an idea of the sensitivity of the energy and angle spectral shape comparison, there was a measured discrepancy in the angular distribution of the e^+-e^- difference which could be accounted for by a 0.02-mrad shift between the e^+ and e^- data. This small discrepancy is consistent with the residual error remaining from the 0.5-mm accuracy with which the beam could be positioned, assuming that the twelve settings at each polarity gave a random error.

Integrated over the whole acceptance, this angular discrepancy contributes only a 0.1% systematic error in the e^+/e^- ratio, and no correction has been made for it. Run-to-run fluctuations in the measured cross sections also show

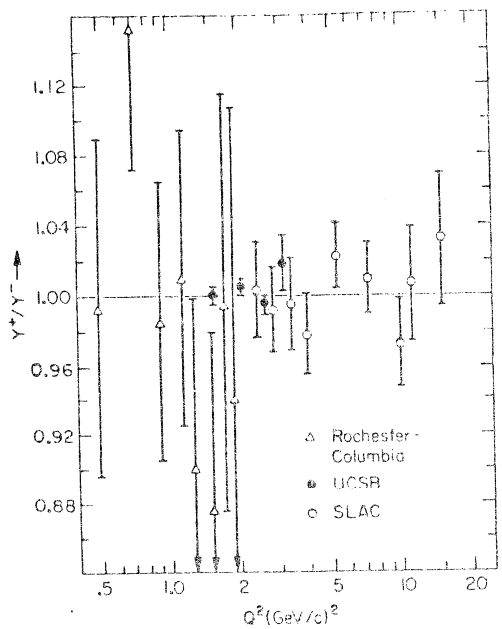

FIG. 2. Ratio (R) of antilepton to lepton inelastic scattering from hydrogen as a function of square of four-momentum transfer (Q^2) for all three reported experiments.

this effect of the setting error, and they give the same 0.1% systematic error. Uncertainties in the $\pi^{\pm}$ contamination correction also give about a 0.1% error, as does the e^+-e^- difference in the empty-target correction, which is due to a difference in the beam halo. A possible asymmetry in the magnetic field settings contributes $< 0.14\%$. Other systematic effects which have been estimated and which each contribute considerably less than 0.1% include beam rate effects, differences in the quantameter response to e^+ and e^-, differences in e^+ and e^- radiative corrections, beam size differences, magnetic effects on phototubes, contribution of high-energy δ rays to the e^- yield, and differences in the e^+ and e^- beams with regard to energy, time distribution, or contamination.

Combining these independent systematic errors with the statistical uncertainly of 0.25% for the data integrated over the range $1.2 < |q^2| < 3.3$ (GeV/$c)^2$ and $2 < \nu < 9.5$ GeV, we get as the main result of the experiment the ratio of cross sections, $e^+/e^- = 1.0027 \pm 0.0035$. This represents a considerable improvement in the accuracy of such particle-antiparticle comparisons for either elastic or inelastic lepton-nucleon scattering and begins to get into the region of accuracy where the absence of two-photon effects might be puzzling. This

TABLE I. Measured corrected (for empty target and pion contamination) yields of e^+ (Y_+) and e^- (Y_-) and their ratios in bins of $Q^2 = -q^2$, the four-momentum transfer. Errors shown are statistical only and radiative corrections have not been applied.

Q^2 (GeV/$c)^2$	Y_+	Y_-	Y_+/Y_-
1.3–1.8	227 054 ± 784	227 010 ± 729	1.0002 ± 0.0047
1.8–2.3	287 029 ± 804	285 228 ± 780	1.0063 ± 0.0039
2.3–2.8	167 359 ± 579	167 997 ± 583	0.9962 ± 0.0049
2.8–3.3	20 148 ± 210	19 766 ± 214	1.0191 ± 0.0150

cross-section ratio is approximately $1 + 4\,\mathrm{Re}(A_2/A_1)$, where A_1 and A_2 are, respectively, the one- and two-photon exchange amplitudes.

Since e^+-e^- differences are likely to be a function of q^2, the four-momentum transfer, we show our data (in terms of corrected yields, $Y_{\pm}$) in binds of 0.5 (GeV/$c)^2$ in Fig. 2 and Table I versus $Q^2 = -q^2$. There is no trend in the data. Our data are given in terms of yields $(Y_{\pm})$ corrected for empty-target counts and pion contamination, but are not radiatively corrected, since the difference in the e^+ and e^- radiative correction is so small. Also shown in Fig. 2 are results[2] from the Rochester-Columbia experiment with muons, and from a SLAC spectrometer experiment which was done at the same time as the work reported here. All three existing sets of inelastic data are plotted with statistical errors only. We have also looked for some dependence of e^+/e^- on ν, the energy transfer from the lepton to the proton, but there is no significant trend.

We wish to thank W. K. H. Panofsky and J. Ballam and the many operating and service people at SLAC for help in making the experiment and its analysis successful, with particular thanks to T. Fieguth for assistance in setting up the beam and Group F for the loan of the quantameter. The assistance of T. B. Risser in the early stages of the experiment is gratefully acknowledged.

*Supported in part by the U. S. Energy Research and Development Administration.

†Present address: Varian Associates, 611 Hansen Way, Palo Alto, Calif. 94303.

[1]S. Hatwig, F. H. Heimlich, G. Huber, E. Rössle, M. Köbberling, J. Moritz, K. H. Schmidt, D. Wegener, D. Zeller, and J. Bleckwenn, Lett. Nuovo Cimento 13, 30 (1975), and eight other references therein.

[2]H. Jöstlein, I. J. Kim, K. Königsman, A. C. Melissinos, P. Mühlemann, E. Aslanides, and P. Limon,

Phys. Lett. 52B, 485 (1974); L. S. Rochester, W. B. Atwood, E. D. Bloom, R. L. A. Cottrell, D. H. Coward, H. DeStaebler, M. Mestayer, C. Y. Prescott, S. Stein, R. E. Taylor, and D. Tines, Phys. Rev. Lett. 36, 1284 (1976).

[3]P. M. Fishbane and R. L. Kingsley, Phys. Rev. D 8, 3074 (1973); G. T. Bodwin and C. D. Stockham, Phys. Rev. D 11, 3324 (1975).

[4]J. C. Pati and A. Salam, Phys. Rev. Lett. 32, 1083 (1974), and Phys. Rev. D 10, 275 (1974).

[5]In a separate experiment using a mixed pion-electron beam, we measured the efficiency of our shower detector for counting pions of various energies. This information was used along with measured pion electroproduction cross sections to predict in a Monte Carlo calculation the pion contamination. The Monte Carlo agreed with the magnet reversed measurement to 13%.

[6]E. D. Bloom, D. H. Coward, H. DeStaebler, J. Press, G. Miller, L. W. Mo, R. E. Taylor, M. Breidenbach, J. I. Friedman, G. C. Hartmann, and H. W. Kendall, Phys. Rev. Lett. 23, 930 (1969), and fits to the data supplied by W. B. Atwood.

Measurement of e^+-e^- Asymmetry in Deep-Inelastic Bremsstrahlung*

D. L. Fancher,† D. O. Caldwell, J. P. Cumalat, A. M. Eisner, T. P. McPharlin,‡ R. J. Morrison, F. V. Murphy,§ and S. J. Yellin

Department of Physics, University of California, Santa Barbara, California 93106

(Received 28 February 1977)

We have measured $(e^+p\to e^+\gamma X)/(e^-p\to e^-\gamma X)=1.080\pm0.036$ in the scaling region, despite our finding e^+ and e^- total inelastic scattering to be the same to the $\frac{1}{3}\%$ level. The magnitude and sign of the difference signal are consistent with the parton model, from which we extract a mean sum of cubes of parton charges in the proton, $\langle\sum_i Q_i^3\rangle=0.89\pm0.34$. Statistics are insufficient to distinguish between fractional ($\langle\sum_i Q_i^3\rangle=0.56$) and integral charge ($\langle\sum_i Q_i^3\rangle=1$, or 0.78 for colored quarks).

Despite the great success of the quark-parton model,[1,2] particularly in understanding leptonic processes, there have been experiments[3-5] involving inelastic Compton scattering which appear to disagree with that model. Many more photons are produced than would be expected from Compton scattering off single partons in the proton, whether for quark or integral parton charges. This photon excess could be due to the decay of unknown hadronic states, the domination[5] of photon dissociation into a parton-antiparton pair over the parton Compton scattering process which had been expected[6] to yield the parton charge, the existence of partons of large charge,[7] or the failure of the model. We report here an experiment which helps to resolve this problem by checking the parton model and the parton charge. The experiment is a measurement of the difference between electron-proton and positron-proton inelastic scattering in which an energetic photon is produced. The first two of the explanations for the inelastic Compton results are irrelevant to this difference measurement: *All* hadronic processes must subtract out, and the photon dissociation process cannot contribute to such an interference.[8] Although the results of this short experiment are not precise enough to distinguish fractional from integral charges for the partons, they are consistent with the parton model for reasonable charge values. The problem with the inelastic Compton scattering results is thus most likely not associated with a failure of the quark-parton model, but rather (as suggested by the constituent interchange model[9] and our previous work[5]) is probably due to the photon dissociation process.

This experiment, which was suggested by Brodsky, Gunion, and Jaffe,[10] is an attempt to measure the interference between the Bethe-Heitler bremsstrahlung amplitude and the virtual Compton amplitude, as shown in Fig. 1. It is seen in these diagrams that one photon interacts with a parton in the Bethe-Heitler case, and two photons interact with a single parton in the Compton case, so that in taking the square, the interference term [Fig. 1(c)] is effectively a three-photon interaction with the parton and depends on the cube of the parton's charge. Only the interference term has odd charge conjugation, and hence it is measurable by taking the e^+-e^- difference. It defines a structure function, V, through the equation,

$$\frac{d\sigma(e^+p\to e^+\gamma X)}{dp_0'd\Omega_e'dk_0d\Omega_k}-\frac{d\sigma(e^-p\to e^-\gamma X)}{dp_0'd\Omega_e'dk_0d\Omega_k}=\frac{\alpha^3p_0'k_0|T_{\rm int}|^2V(x')}{2\pi^2M_pp_0(-q^2)},\qquad(1)$$

where M_p, p_0, p_0', and k_0 are the energy components of the four-vectors shown in Fig. 1, Ω_e,

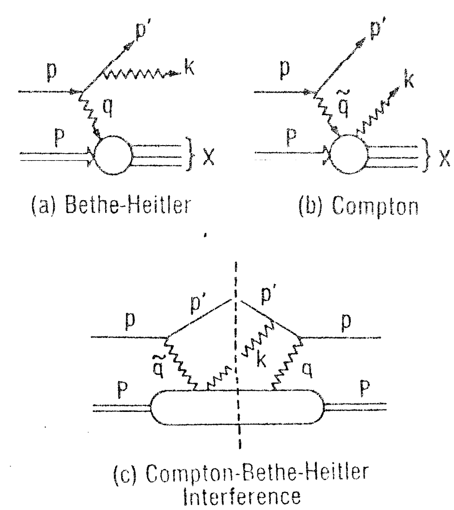

FIG. 1. Diagrams for the reaction $e^\pm+p\to e^\pm+\gamma$ + anything.

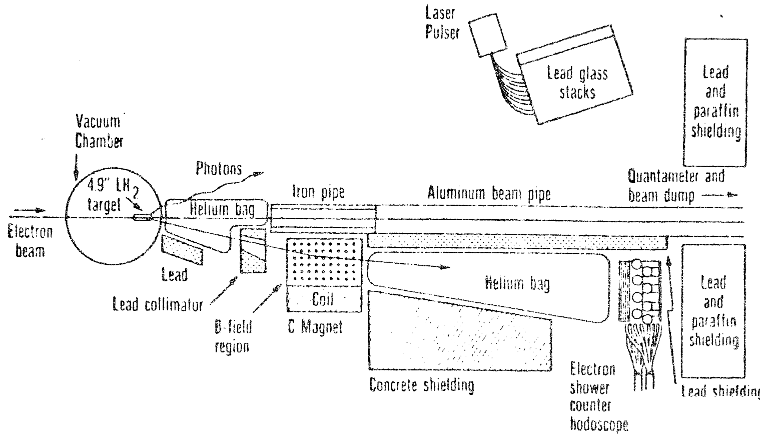

FIG. 2. Schematic experimental layout for the experiment.

and Ω_k are the solid angles for the outgoing $e^\pm$ and photon, $x' = -q^2/(2P\cdot q + M_p^2)$, and $T_{\rm int}$ is a known interference amplitude. In a parton model, V depends on the single kinematic variable, x', and has the form $V(x') = \sum_i Q_i^3 u_i(x')$, where $u_i(x')$ is the probability per unit x' that the proton contains a parton of charge Q_i with fraction x' of the proton's momentum in an infinite-momentum frame. For comparison, the structure function νW_2 determined in inelastic lepton scattering has the form $x' \sum_i Q_i^2 u_i(x')$.

Since the run was limited to only 200 h, we could not determine $V(x')$. However, we did get some measure of $\int_0^1 V(x')dx' = \langle \sum_i Q_i^3 \rangle$. This exact sum rule[10] would give $\langle \sum_i Q_i^3 \rangle = \frac{5}{9}$ for fractionally charged quarks (independent of the presence of gluons or quark-antiquark pairs), or 1 if all partons have charge 0 or ± 1, or $\frac{7}{9}$ for integrally charged colored quarks below the color threshold[11] (because there is a color-octet contribution to intermediate states in the Compton diagram).

The experimental apparatus used to measure the e^+-e^- difference was a two-arm spectrometer, as shown in Fig. 2. The electron arm, made up of a magnet, lead-scintillator hodoscope, and some auxiliary counters, was set at a mean angle of 8° from the beam line. It had an acceptance of 3.1 msr in solid angle and 4 to 11.5 GeV in energy and is described in more detail elsewhere.[12]

The photon arm consisted of two stacks of SF2 lead-glass counters, one made up of forty counters, each $6.4 \times 6.4 \times 34.3$ cm^3, and the other consisting of 48 counters, each $6.4 \times 6.4 \times 58.4$ cm^3. The two stacks, which were arranged in a fly's-eye configuration, pointed at the 12.5-cm hydrogen target at a mean angle of about 7°, subtended a solid angle of 8.8 msr, and covered an energy range of 2 to 8 GeV. The kinematic region covered in the experiment is shown in Table I.

The nearly identical electron and positron beams were both made one-third of the way down the Stanford Linear Accelerator and then accelerated to 13.5 GeV. The polarity was alternated periodically to minimize systematic errors, and about equal amounts of data were collected at three intensities (3, 5, and $7\times 10^7 e^\pm$ per 1.6 μsec pulse) so as to monitor rate effects, which turned out to be unimportant. A total of 3.23 $\times 10^{15}$ incident $e^\pm$ were used. The electron beam is discussed in more detail elsewhere.[12]

Whenever a signal in the $e^\pm$ arm was larger than 3.8 GeV, all lead-glass blocks and hodoscope elements were pulse-height analyzed. When there was also a signal in the photon arm, the relative time between the $e^\pm$ trigger and the photon was also measured and recorded on magnetic tape. In addition to this data information, pulse heights in the lead-glass blocks and hodoscope elements in response to light pulses were also periodically recorded to help maintain the basic calibration,

TABLE I. Kinematic range covered by the experiment for variables defined in Fig. 1, except $x' = -q^2/(2P\cdot q + M_p^2)$.

Variable	Range
$-\tilde{q}^2$	1.5–3.3 (GeV/c)^2
$\tilde{q}_0$	2–9.5 GeV
$-q^2$	0.75–2.0 (GeV/c)^2
k_0	2–8 GeV
x'	0.12–1.0

which was done with e^+ of known energy.

In addition to normal data runs and empty-target runs, some information was obtained with the magnet polarity of the $e^\pm$ arm reversed from that of the incident beam. For example, to measure the effect of π^+ simulating an e^+ in the trigger, we ran with an e^- beam but with the spectrometer magnet set for e^+ and assumed that the e^- produced as many π^+ as the e^+ beam would have.

To get an idea of the sensitivity required in the experiment, the anticipated size of the e^+-e^- difference in Eq. (1) is of the order of 0.2 nb/GeV^2 sr^2, and our acceptance was $\Delta p_0'\Delta\Omega_e'\Delta k_0\Delta\Omega_k \approx 0.0007$ GeV^2 sr^2. Thus the signal was small. We detected 2366 events of the type $e^+p\to e^+\gamma X$ and 2161 events of the type $e^-p\to e^-\gamma X$. After correcting these numbers for π contamination, we found

$$\frac{N(e^+p\to e^+\gamma X)}{N(e^-p\to e^-\gamma X)}=1.080\pm0.036. \qquad (2)$$

This ratio would be unity if the photons came from π^0 decays or any other hadronic process. In fact, most of the events were due to electroproduced π^0's, which subtract out in the difference, but which tend to wash out the sought-after asymmetry in the ratio.

This result, (2), applies to those events which are likely to lie in the scaling region, because the following cuts have been applied: $|\tilde{q}^2|\geq 1.5$ (GeV/c)^2, $|q^2|\geq 0.75$ (GeV/c)^2, and $|\tilde{q}^2-q^2|\geq 0.75$ (GeV/c)^2, where q and $\tilde{q}$ are defined in Fig. 1. These cuts are meant to insure that the three-photon interactions of the interference term are with the same parton, and that the partons can be treated as free during the interaction.[10] The cuts are a little less stringent than advocated in Ref. 10, but we have used the variable x' which gives scaling at smaller $|q^2|$ values than does $x=-q^2/2P\cdot q$, which is used in Ref. 10. Other kinematic constraints of that reference are automatically satisfied by the acceptance of our apparatus.

A systematic error could arise from possible gain changes in the counters in the electron or photon arm when the magnetic fields were reversed. We have several reasons for believing that we have essentially no error from this source: (1) Our light pulser calibration system enabled us to correct for such gain changes (typically $<3\%$). (2) Monte Carlo studies showed that the observed gain changes would have been too small to account for our observed asymmetry, even if we had not corrected for them. (3) In the case of the photon arm, it would take at least an 8% gain difference in order to produce the observed asymmetry. However, such a difference would cause an 8% difference in the measured mass of those π^0's for which both decay photons entered the photon arm. Less than 1% mass difference was observed. (4) In the case of the electron arm, our simultaneous measurement[12] of the ratio

$$\frac{N(e^+p\to e^+X)}{N(e^-p\to e^-X)}=1.0027\pm0.0035. \qquad (3)$$

provides evidence that the $e^\pm$ arm was equally sensitive to electrons and positrons.

This comparison of inelastic electron and positron scattering serves two other purposes. First, the e^+ and e^- beams were sufficiently alike so as not to affect the asymmetry of Eq. (2). Second, this lack of two-photon exchange effects in the total cross section makes it unlikely that such effects could contribute to that asymmetry.

Another check on the behavior of the photon side, in addition to the one given by comparing the masses of the π^0's produced by e^+ and e^-, is provided by comparing the number of π^0's detected with each beam polarity. That number was the same within the statistical error for the 400 π^0's for which we could measure both photons.

Since an e^+-e^- difference of the correct sign and a reasonable magnitude was observed, we sought an estimate of $\langle\sum_i Q_i^3\rangle$ from the data. To do this we weighted each event by a function which was largest in kinematic regions where we expected a large interference term and a small π^0 background. The result of such a weighting leads to an unbiased estimate of $\int_0^1 V(x')dx'$, provided that a shape, but not a normalization of $V(x')$, is assumed. The shape assumed was

$$V(x')\propto x'^{-1/2}(1-x')^3(1+2.5x'), \qquad (4)$$

which is very close to the $V(x')$ that one would compute from the modified Kuti-Weisskopf quark distribution,[13,14] and which was designed to fit deep-inelastic lepton scattering data.

The result of this procedure was

$$\langle\textstyle\sum_i Q_i^3\rangle=\int_0^1 V(x')\,dx'=0.89\pm0.34. \qquad (5)$$

In getting this result we made the small corrections (which were close to the same for both polarities) for $\pi^\pm$ contamination ($\sim3\%$) and empty-target events ($\sim10\%$), but neglected the effect of accidentals ($\sim15\%$), since the beam intensities at the two polarities were well controlled, and examination of out-of-time (o.t.) e-γ coincidences gave

$$\frac{N(e^+p \to e^+\gamma X)_{\text{o.t.}}}{N(e^-p \to e^-\gamma X)_{\text{o.t.}}} = 1.00 \pm 0.08. \quad (6)$$

Systematic uncertainties occur in the conversion of the observed asymmetry into an estimate of $\langle \sum_i Q_i^3 \rangle$. For example, we used $|T_{\text{int}}|^2$ of Ref. 10 as computed for partons of spin $\frac{1}{2}$, but when $|T_{\text{int}}|^2$ for spin-0 partons was used, the result increased $\langle \sum_i Q_i^3 \rangle$ by only 5%. More serious was the uncertainty in the assumed shape of $V(x')$. When we used an alternative parton distribution,[15] also like (4) in that it was designed to fit the lepton scattering data, we obtained a result only 7.5% higher than that presented in (5). Both shapes for $V(x')$ become infinite as x' goes to zero. When we tried $V(x') \propto x'(1-x')^3$, which goes to zero when x' becomes zero and which is not designed to fit other experimental data, our result (which went down to $x' = 0.12$) decreased by 26%. The spread in these values gives some idea of the systematic error to be expected from the assumption of a shape for $V(x')$.

In conclusion, we have found an asymmetry between $e^+p \to e^+\gamma X$ and $e^-p \to e^-\gamma X$. The resulting estimate, $\langle \sum_i Q_i^3 \rangle = 0.89 \pm 0.34$, while not statistically precise enough to distinguish between fractional and integral parton charge, does support models with partons of low charge, since $\int V(x')dx'$ would have had a big value if partons had the large charges needed if this were the explanation of the inelastic Compton results, or it could have any arbitrary positive or negative value if the parton model were wrong.

We wish to thank T. B. Risser who made important contributions to this experiment in its earlier stages. We have benefitted from discussions with several theorists, but particularly S. J. Brodsky and M. S. Chanowitz. The help of many people at Stanford Linear Accelerator Center is gratefully acknowledged.

---

*Supported in part by the U. S. Energy Research and Development Administration.

†Present address: Lawrence Berkeley Laboratory, University of California, Berkeley, Calif. 94720.

‡Present address: High Energy Physics Laboratory, Stanford University, Stanford, Calif. 94305.

§Present address: Varian Associates, 611 Hansen Way, Palo Alto, Calif. 94303.

[1] R. P. Feynman, *Photon-Hadron Interactions* (Benjamin, New York, 1972).

[2] V. Barger and R. J. N. Phillips, Nucl. Phys. B73, 269 (1974), and references therein.

[3] B. W. Worster *et al.*, Lett. Nuovo Cimento 5, 261 (1972).

[4] J. F. Davis *et al.*, Phys. Rev. Lett. 29, 1356 (1972).

[5] D. O. Caldwell *et al.*, Phys. Rev. Lett. 33, 868 (1974).

[6] J. D. Bjorken and E. A. Paschos, Phys. Rev. 185, 1975 (1969).

[7] P. C. M. Yock, Int. J. Theor. Phys. 2, 247 (1969), and Ann. Phys. (N.Y.) 61, 315 (1970).

[8] S. J. Brodsky, private communication.

[9] R. Blankenbecler and S. J. Brodsky, Phys. Rev. D 10, 2973 (1974).

[10] S. J. Brodsky, J. F. Gunion, and R. L. Jaffe, Phys. Rev. D 6, 2487 (1972). Note that there is a problem with experimentally evaluating their sum rule, as is discussed by R. J. Morrison (to be published), and hence we did not use this approach.

[11] M. S. Chanowitz, Lawrence Berkeley Laboratory Report No. LBL-5312, 1976 (unpublished), and private communications.

[12] D. L. Fancher *et al.*, Phys. Rev. Lett. 37, 1323 (1976).

[13] J. Okada *et al.*, University of Hawaii Report No. 511-209-76, 1976 (to be published).

[14] R. McElhaney and S. F. Tuan, Phys. Rev. D 8, 2267 (1973).

[15] R. Blankenbecler *et al.*, SLAC Report No. SLAC-PUB-1531, 1975 (unpublished).

SLAC PROPOSAL E-124 suppl. 1
Received December 28, 1976

A Three-Photon Measurement of Parton Charge and Search for Color

Submitted by

University of California at Santa Barbara

D. O. Caldwell, A. M. Eisner, A. Lu, R. J. Morrison, and S. J. Yellin

University of California at Davis

J. H. Klems, W. T. Ko, R. L. Lander, and D. E. Pellett

and

University of California at San Diego

G. E. Masek and E. Miller

December 1976

I. INTRODUCTION TO THIS REVISED PROPOSAL

In April 1976 we submitted a proposal to perform an experiment which could (1) provide a crucial test of the parton model, (2) determine whether partons have fractional or integral charge, and (3) in the latter case show whether "color" exists. We had completed a 200-hour trial (E-99) of that experiment and had shown that the effect sought, a difference between $e^- + p \rightarrow e^- + \gamma$ + anything and $e^+ + p \rightarrow e^+ + \gamma$ + anything, did indeed exist with the correct sign and magnitude. The limited statistics of that experiment precluded achieving the goals mentioned above, but we felt the proposed experiment could have done so.

That proposal was deferred primarily because the EFD and running time costs to SLAC were judged to be high, and the proposal was not complete enough to justify committing those resources. Now we understand the situation to be even worse, with both an extremely low pulse utilization projected and with EFD equipment money for Fiscal 1977 already allocated mostly for projects not related to the conventional linear accelerator program. Despite this gloomy outlook, we feel that the physics to be done is so worthwhile that it is necessary to propose an experiment of a somewhat radical form which might satisfy SLAC's fiscal constraints. We were pleased to find that this new way to do the experiment is not only much less demanding on SLAC, but also can produce a more accurate result in a shorter time than in the previous proposal, provided the "Lead Glass Wall" is available to us. Both because of the altered form of the experiment and because personnel on the Program Advisory Committee have changed, we are submitting a new proposal. Some of the background material is the same as in the previous proposal, however.

II. GOALS OF THE EXPERIMENT

The primary goal of the experiment is to measure the difference in energetic photon production by electrons and by positrons. The use of this difference to provide a stringent test of the parton model and to measure the mean-cubed parton charge will be discussed in the next section, where the necessary theoretical background is given.

Here we shall be concerned with secondary goals, one of which is to extend our comparison of inelastic e^- and e^+ scattering to larger values of the square of the four-momentum transfer, q^2. In the previous experiment (E-99) we found[1] over the range of virtual photon kinematics, $1.2<|q^2|<3.3\,(\text{GeV}/c)^2$, $2 < \nu < 9.5$ GeV, $e^+ + p \to e^+ + \text{anything}/e^- + p \to e^- + \text{anything} = 1.0027 \pm 0.0035$ (including statistical and systematic errors). The lack of two-photon exchange effects to this level of accuracy is perhaps surprising, but in addition this result has two consequences for the main experiment: (1) two-photon interference effects cannot be responsible for the difference (of the order of 10%) we observed in the real photon production channel, and (2) this provides proof of no experimental biases in the e^+ and e^- detection which could affect the difference we observe in γ production.

In the proposed experiment we would obtain simultaneously with the photon production data an extension of the accurate comparison of e^+ and e^- deep inelastic scattering to larger values of q^2, where differences are more likely to appear. The planned range of q^2 covered would be increased by a factor of more than three. In that higher range of q^2 the accuracy of the measurement should exceed our previous effort. Besides better statistics, systematic errors will be reduced which result from the beam location and halo. The beam location accuracy will not only be improved with a microwave beam centering device, but also the proposed symmetric apparatus will be much less sensitive to this error. Perhaps at last some two-photon exchange effect could be seen.

We are just finishing the analysis of another experiment (E-88) done continguously with E-99 and performed with the same apparatus, and again more information on the same process could be obtained simultaneously. This experiment measured deep inelastic π^o electroproduction, and the results can be interpreted as providing further information on the parton structure of the photon and of the proton. For instance, the electroproduced π^o's have a mean transverse momentum which becomes independent of $|q^2|$ in the range of 2 to 8 $(GeV/c)^2$ and of a value like that found in hadronic processes. The longitudinal momentum distribution is also quite similar to that found in e^+-e^- annihilation or in hadronic collisions. Both results are consistent with the virtual photon's interacting with a parton, which then produces a hadronic "jet", the nature of which is independent of the incident particle. This is unlike the behavior we found for real photons (in π^o photoproduction[2]) which appear (in at least one kinematic region) to dissociate into a parton-antiparton pair, which subsequently interact with partons in the nucleon to produce two "jets". Substantiation of the above picture of virtual photon-parton interactions is provided by the flat π^0 azimuthal dependence, the π^0 cross section's being close to the average of the π^+ and π^-, and by the dependence of the π^0 cross section on center-of-mass energy.

The proposed experiment would have both a considerably increased efficiency for π^0 detection and an increased kinematic range, particularly permitting measurements farther into the deep inelastic region. This would provide an extension of the previous work in accuracy, as well as in q^2 and transverse momentum. Tests not previously possible would become feasible, such as detailed comparisons with the Constituent Interchange Model, and a possible way to measure the transverse momentum distribution of partons in the proton. Another interesting possibility is a more direct comparison between the interaction of real and virtual photons over a similar kinematic range, since we would plan to spend about 100 hours using a photon beam, mainly for checks having to do with the primary goal of the experiment. However, this would also provide π^0 and η^0 photoproduction data over a larger kinematic range than we achieved in a previous SLAC experiment[2] (E-76). We could even check out to larger values of transverse momentum, our previous[3] peculiar result of an extraordinarily large deep inelastic Compton scattering.

The photon beam run could in addition provide an interesting search for high-mass particles which decay into photons, electrons, or π^0's. We ought to be able to get up to masses approaching SLAC's kinematic limit (~ 6 GeV/c^2). In 100 hours we could get down to $\sim 10^{-4}$ of the $\psi \rightarrow e^+ + e^-$ cross section, so the search could be a rather definitive one. Since part of SLED will be operational in the Fall of 1977, with reduced beam intensity and SLED we could extend this search to even higher masses.

III. THEORETICAL BACKGROUND FOR THE $e^+ - e^-$ DIFFERENCE MEASUREMENT

Brodsky, Gunion, and Jaffe[4] suggested that a difference could arise between the e^+ and e^- cross sections for deep inelastic electroproduction of photons from an interference between the Bethe-Heitler bremsstrahlung amplitude and the virtual Compton amplitude. These two processes are shown in Fig. 1. If the proton is considered to be made of partons, it is seen from these diagrams that one photon interacts with a parton in the Bethe-Heitler case and two photons interact with a parton in the Compton case, so that in taking the square, the interference term (Fig. 1c) is effectively a three-photon interaction with the parton. The interference or difference term then has odd charge conjugation and depends on the cube of the parton's charge.

Specifically, the difference of the positron and electron cross sections in the deep inelastic region determines a structure function

$$V(x) = \sum_a \lambda_a^3 \, U_a(x), \qquad (1)$$

where $U_a(x)$ is the probability of finding a parton of type "a" with charge λ_a and fraction x of the proton's momentum in an infinite momentum rest frame. Note that V(x) depends on only one (x) of the six kinematic variables needed to specify the process. This scaling with x alone provides a very stringent test of the parton model and checking just this feature would be sufficient justification for the experiment.

Furthermore the measured $V(x)$ helps determine $U_a(x)$, which has been sought in inelastic electron, muon, and neutrino experiments. In principle the present experiment is the cleanest way to determine the valence quark part of $U_a(x)$. Because of the odd charge conjugation there are no Pomeron contributions arising from the quark-antiquark sea in this process. Thus this experiment ought to shed further light on the behavior of valence quarks, provided $V(x)$ scaling is observed. It could provide a test of p-quark dominance without the ambiguities of the inelastic electron scattering from deuterium.

If one could measure over all x values from 0 to 1, then the parton charge could be determined without any knowledge of $U_a(x)$ by using an exact sum rule. The point is that $Q=\int_0^1 dx \sum_a \lambda_a U_a(x)$ $Y = \int_0^1 dx \sum_a y_a U_a(x)$, and $B = \int_0^1 dx \sum_a b_a U_a(x)$ are the charge, hypercharge, and baryon number of the target parton of interest, and because it has odd charge conjugation, λ_a^3 can be reduced to a linear combination of λ_a, y_a, and b_a. Thus the integral $\int_0^1 V(x)dx = \int_0^1 dx \sum_a \lambda_a^3 U_a(x)$ is determined just by quantum number conservation. If the parton charge is 0 or ±1, $\lambda_a^3 = \lambda_a$, so

$$\int_0^1 V(x)dx = Q = \begin{cases} 1 \text{ for protons} \\ 0 \text{ for neutrons} \end{cases}, \qquad (2)$$

and for fractionally charged quarks, $\lambda_a^3 = \frac{1}{3}\lambda_a + \frac{2}{9} b_a$, so

$$\int_0^1 V(x)dx = \frac{1}{3} Q + \frac{2}{9} B = \begin{cases} 5/9 \text{ for protons} \\ 2/9 \text{ for neutrons} \end{cases}. \qquad (3)$$

Note that an even charge conjugation process, such as inelastic electron scattering, does not lead to an exact sum rule for the charge. Furthermore, if neutral gluons are present, the inexact sum rules obtained give an erroneously low charge value. The three-photon process considered here is completely insensitive to the presence of gluons.

Recently Chanowitz[5] has added an exciting new reason for doing this experiment, the possible detection of "color". Below the color threshold the electromagnetic current has only color singlet interactions, and hence quarks would display fractional charge. However, in some two-photon processes where the current comes in as the square, a color octet piece is projected out. The existence of color is then shown by the increase in the mean cubed charge, resulting in

$$\int_0^1 V(x)dx = 7/9, \qquad (4)$$

for integrally charged quarks below the color threshold. This, then, is a specific and very important reason for doing this experiment at SLAC energies.

However, this sum rule suffers from the same problem similar quark sum rules do, namely that most partons have small x values, and it is difficult to make measurements to small enough values of x. In the small x region there can be a Reggeon-exchange contribution with an integrable $x^{-1/2}$ singularity. One can obtain[6] a limit on the contribution to $\int V(x)dx$ from the large x region by noting that

$$\nu W_2^{ep}(x) = x \sum_a \lambda_a^2 \, U_a(x) \tag{5}$$

and getting an upper bound from assuming that only the p (or up) quark contributes with its charge of + 2/3. Thus

$$\frac{2}{3} \int_{x_o}^{1} \frac{\nu}{x} W_2^{ep}(x)dx > \int_{x_o}^{1} V(x)dx. \tag{6}$$

The measurable lower limit, x_o, depends on how small a value of q^2 (see Fig. 1) one can use and still get scaling, and only the experiment can determine that. However $x_o = 0.05$ is an absolute limit, and if $x_o = 0.15$, then >54% of $\int_o^1 V(x)dx$ is not measurable,[6] if the whole integral is equal to 5/9. Thus there are two ways to do the experiment: (1) measure to sufficiently small x so that the data can be extrapolated to x = 0, knowing the $x^{-1/2}$ dependence, which is fortunately possible because there can be no x^{-1} Pomeron contribution, or (2) use the larger x region where the quark charge is given from the ratio of V(x) to $\nu W_2/x$ to a good approximation. The inelastic scattering results (eq. 5) depend on λ^2, and the difference experiment (eq. 1) depends on λ^3, so the ratio determines λ, particularly for p-quark dominance. This comparison could even be extended down to moderately small x by correcting for the small Pomeron contribution to eq. 5. Obviously both approaches would be used, but the success of the first depends on getting scaling to small enough x so that the trend of V(x) is well enough established to make a meaningful extrapolation, and there is no way of guaranteeing the accuracy of that procedure at this stage, if partons have fractional charge. If the charge is integral, there is not such a large contribution at small x, and in any case it will be possible to show (method 2) that the bound of eq. 6 is exceeded for the fractionally-charged quark model. Thus this otherwise unfortunate development would then provide a powerful way of proving that the charges are integral.

IV. PREVIOUS EXPERIMENT (E-99)

Using apparatus (Fig. 2) originally designed for an experiment (E-88) on deep inelastic π^0 production, the UCSB group used 200 hours of accelerator time to check out and try the three-photon experiment. As can be seen from the figure, there was a stack of 88 lead glass counters (of 2 1/2" x 2 1/2" cross section) on one side of the 13.5-GeV e^+ or e^- beam, and a recoil electron detector on the other side. The electron detector consisted of a bending magnet and a hodoscoped lead and scintillator shower detector, which could be moved into the main beam for calibration. The shower detector determined the energy and position of the electron, which permitted tracing the electron trajectory back through the magnet to the small target, giving the production angle. As a check, many of the electrons also went through a thin hodoscope at the exit of the magnet, giving a second electron position and hence determining the momentum. This latter over-determination also provided a check on the pion contamination of

2-3%, which was measured in two other ways, all of which agreed. One measurement involved reversing the bending magnet field with respect to the beam magnets, so as to determine the number of π^+ with e^- incident or π^- with an e^+ beam. Second, with normal fields, sufficient lead was placed in front of the shower detectors to attenuate strongly the electrons, but to admit a known fraction of the pions.

Although a wider range was covered in E-88 by having a higher beam energy and moving the detectors, in E-99 we used a single position and detected electrons such as to give virtual photons of $|q^2|$ from 1.2 to 3.3 $(\text{GeV}/c)^2$ and ν from 2 to 9.5 GeV. Interleaved e^+ and e^- data were collected in equal amounts at three beam intensities (3×10^7, 5×10^7, and 7×10^7 e's/pulse), so that any rate-dependent effects could be monitored. This did not produce any important systematic errors in even the e^+-e^- inelastic scattering difference, nor did beam integration differences with e^+ and e^-, beam diameter differences, beam angle error, quantameter errors, magnetic effects on phototubes, or high-energy δ-rays. In the single-arm experiment, where the statistical error was 0.25%, four sources of systematic error each contributed about 0.1%. One was due to inaccuracies in the correction for pion contamination, there being more π^+ than π^-. Another arose from the lack of reproducibility of the incident beam position; this setting error of about 0.5 mm was random, but it left a residual error. The third was from beam halo differences and could be measured in target-empty runs. The fourth was the limit which could be placed on the accuracy of setting the magnetic field for the two polarities. All of these can be improved or eliminated in the proposed experiment, and all will be unimportant for the e-γ measurements.

For the photon detection experiment, all photons in time coincidence with a suitable electron and having an energy greater than 4 GeV had their pulse heights and arrival times recorded, and all accompanying particles yielding more than 1 GeV were also recorded. With this information, it was relatively straightforward to make good corrections for accidental coincidences, although in principle if one were careful (as we were) to use the same beam intensities, these should subtract out in the e^+-e^- difference. Where the difference subtraction was really important was in eliminating the background from $\pi^0 \to 2\gamma$ decays. That this subtraction was being done correctly could be checked by measuring simultaneously the amount of π^0 production by analyzing those cases in which both photons had sufficient energy to be counted. Within statistics, the number of π^0's produced by e^+ and e^- were the same. It is important to note that <u>all</u> spurious hadronic processes (even the decay of presently unknown particles) must subtract out in this difference.

The result of the e^+ and e^- deep inelastic scattering comparison has been given above. Although that difference was less than 1/3% we did observe a difference in the channel in which an energetic photon was produced, getting $\frac{e^+ \to \gamma}{e^- \to \gamma} = 1.11 \pm 0.04$. In principle the mean cube of the parton charge could then be determined through integrating over V(x), which is given by

$$V(x) = \frac{\sigma_+ - \sigma_-}{\pi^2 \alpha^3 s(-q^2)\,|T_{int}|^2} \qquad (7)$$

where $\sigma_+ = \dfrac{d^6\sigma(e^+p\to e^+\gamma X)}{\frac{d^3p'}{p_0}\,\frac{d^3k}{k_0}}$ and $\sigma_- = \dfrac{d^6\sigma(e^-p\to e^-\gamma X)}{\frac{d^3p'}{p_0}\,\frac{d^3k}{k_0}}$, and where the various kinematic quantities are defined in Fig. 1 (with the subscript 0 indicating the energy part of the corresponding four-momentum), and $|T_{int}|^2$ is a known electrodynamic function arising from the interference of the Bethe-Heitler and Compton amplitudes. However, the small x problem discussed in the previous section makes the charge determination model dependent, because the data neither goes to very small x nor has good enough statistics. The result of this short run is a mean-cubed charge of 0.88±0.34, where the errors are statistical and do not include the uncertainty in extrapolating to small x values. While this result does not distinguish between 0.56 for fractional charge and 0.78 for integral charge below the color threshold, the observation of the right sign and magnitude of the effect is a confirmation of the theoretical ideas and calls strongly for further measurements.

V. DIFFERENCES BETWEEN THE PREVIOUS AND PROPOSED EXPERIMENTS

In the proposed experiment we should like to get nearly an order of magnitude improvement in statistics, as well as to reduce some potential systematic errors. In our April 1976 proposal we discussed a system of the same type but much larger than that used in the E-99 experiment just described. This required a large bending magnet, and it has subsequently been determined that none of those available at SLAC are suitable. We designed one with a desirable form, but its cost (~\$100,000) appears to preclude this way of doing the experiment in the time period of interest. Instead we are now proposing an unusual set-up which does not have any magnet at all. Apart from the fiscal constraints which forced us in this direction, the new arrangement has some important advantages, particularly in eliminating systematic errors and in improving counting rates.

Perhaps the most potentially damaging systematic error for at least some magnet systems would be charged pion contamination. Although the shower detectors give a large apparent energy only rarely for charged pions, the inequality in numbers of π^+ and π^- could introduce a false asymmetry in the e-γ measurement, if charged pions were only partially swept out by a magnetic field. Thus unless an extremely powerful magnet were used, it is better not to sweep magnetically the γ detector. It is probably obvious that beam rates are such that scintillation detectors cannot be used to separate charged from neutral particles.

Achieving large solid angles is difficult while providing magnetic analysis on the electron side and a field-free region on the photon side. The magnet designed could be described as a cross between a C and an H magnet. However, if there is no magnetic analysis, this problem does not arise. The idea is to have a very large shower detector with a hole in the middle, so that all azimuthal angles of e's and γ's can be detected. One cannot then distinguish directly between the two kinds of particles, however. In general the electron's transverse momentum is the greater, since that of the virtual photon is used in producing several particles. This is useful in distinguishing electrons for the auxiliary experiments, since in the region of large $|q^2|$ there is not much contamination of electrons from even π^o mesons. In the main experiment (e-γ) it turns out that the distinction does not have to be made at all. One simply adds the two distributions for the two possible particle assignments and looks for the $e^+ - e^-$ asymmetry. This completely symmetric measurement has the beauty of eliminating most systematic errors. The main errors could arise from beam differences, and this would be accurately checked by the comparison of e^+ and e^- inelastic scattering. A price is paid in a reduction in the magnitude of the asymmetry, but the large solid angle permits a high-statistics subtraction of the two big numbers.

The large solid angle is the key to making all this possible, and that means borrowing the "Lead Glass Wall" after the run with it is completed at SPEAR. We have already been funded by ERDA to purchase about 300 small blocks of lead glass which we would use in the hot region around the central 6^o hole. The size of the hole is chosen to be as large as possible to reduce background counting rates, but not so large as to cut into the desired deep inelastic kinematic region. These blocks would have 2 1/2" x 2 1/2" cross sections and would be surrounded radially outward from the beam by the 6" blocks from the 2m x 2m Lead Glass Wall, as shown in Fig. 3.

Shower locations would not be determined precisely enough, particularly in the big blocks, so the whole array would be backed by proportional chambers, which would measure the showers leaking out the back of these 10-radiation-length blocks. Monte Carlo studies show that the core of the shower is well preserved at these depths, so that its centroid can be located with sufficient accuracy. The showers to be measured are 5-15 GeV, and over this range the results are not very energy dependent. While there is a halo of low-energy photons (~1 MeV), there is a central core of higher energy (~10 MeV) electrons, typically ~15 which remain quite close to the original shower axis. At the exit of the blocks 90% of the electrons are within a 1 cm diameter circle. Even with the photomultipliers on the front end of the blocks -- and studies have shown that this does not degrade energy resolution appreciably -- about 5 cm would be needed to get to the active region of the chambers, at which point the 90% circle has a 5 cm diameter. However, the shower axis can still be located to an accuracy of about 0.7 cm at that distance by averaging the electrons' positions. Thus a considerable improvement is possible over our previous experiment in which the electron position error was 3 cm and the photon error 6 cm. To match this improvement, the energy measurement error must also be improved, and this will automatically occur for the 6" blocks, but will mean energies in adjacent blocks must be added for the 2.5" blocks. This better resolution helps in measuring π^0's and in determining the important kinematic parameter x in the e-γ measurement. For a 2 cm error in shower position, the error in x is $(x + x^2)/20$ and for a 2.5% energy resolution the error is $x^2/5$, both of which are small at small x where V(x) contributes most to the charge determination.

This detector makes feasible our working in End Station A, instead of B, as in the previous proposal. Thus we would then not be incompatible with the bubble chamber or LASS. This would also be cheaper for SLAC, since shielding costs were appreciable for the End Station B set-up. Changing from an electron to a photon beam would also be easier in A. Another advantage would be that the beam dump could be far from the detector and well shielded, so as to avoid back splash in the chambers. Still another positive feature is that the accurate microwave beam positioning device exists in End Station A, as well as suitable beam integrating devices. However, the set-up time is appreciable, and hence using End Station A is sensible if the set up can be done during the long 1977 off time.

The hydrogen target arrangement of End Station A would be satisfactory, and we should like to use a flask of about 5", such as we have had previously. This gives a tolerable 10% empty target contribution, which subtracts out in the e^+-e^- difference anyway, and it provides close enough to a point source so as not to dominate the errors in determining the kinematic quantities.

One remaining item of some cost to SLAC is the introduction of a positron source closer to the beginning of the linac, so that we could use a 20 GeV beam, instead of the 13.5 GeV available last time. For intensities up to about 10^8 electrons per pulse the cost was previously estimated to be $60,000. To keep the beams the same, the positron source is used also as the electron source. The increased energy makes available a larger scaling region and folds the events into the detector more efficiently. At 13.5 GeV it would take about three times as long to get the same statistics as at 20 GeV, and in addition we would lose the lowest x bin and effectively the highest q^2 bin discussed in the next section. For the scaling check at $3 \leq |q^2| \leq 5 (\text{GeV/c})^2$ about 10 times as much running time would be required to get the same statistics.

The higher energy then increases the data rate considerably. Also to improve the data rate we can increase the beam intensity over that for the old experiment by putting half a radiation length of light absorber in front of the detector to reduce low-energy backgrounds which pile up and make errors in shower energy determinations. We have tested such an arrangement and find that it does not appreciably degrade energy resolution.

VI. RATES AND TIME

Previously we requested 1000 hours for an experiment which had less precision in the e^+-e^- difference than the one we are proposing here to do in 500 hours. Of this time, 100 hours would be spent using the photon beam, and the rest divided about equally between e^+ and e^- beams. Considering time for various checks, polarity switch-over time, and the usual inefficiencies and down time, it is safest to quote results expected for 100 hours on each polarity of full efficiency running at 20 GeV with 10^8 electrons per pulse, 180 pulses per second into a 12.5 cm hydrogen target. The Monte Carlo calculations are for detection of photons and electrons between 6^o and 15^o, provided $|q^2| > 1\,(\text{GeV/c})^2$, $|\tilde{q}^2| > 1\,(\text{GeV/c})^2$, and $|\,|q^2| - |\tilde{q}^2|\,| > 1\,(\text{GeV/c})^2$ to keep the data in the scaling region. Table I shows the number of standard deviations from zero the e^+-e^- difference would be for various bins in x and q^2.

These variables do not depend on which particle is the electron and which is the photon. The distribution function to be determined by the measurement, V(x), should depend only on x and not on q^2, and hence the binning also in q^2 indicates how well a scaling check can be made. Another kinematic variable, the mass of the electron-photon system also does not depend on particle assignment, and hence a scaling check in that variable can also be done directly. We could run at 13.5 GeV also, if it appeared especially desirable to check energy scaling. For the remaining variables like $\tilde{q}^2$, the scaling check has to be indirect, but it can be done with the data obtained. The procedure is to assign each event into two bins in $\tilde{q}$ according to the probability that the particle is a photon or an electron, as determined by T_{int} (see the discussion of Eq. 7) and see if V is a function of x alone or x and $\tilde{q}$. We can check over the range $2 \leqslant |\tilde{q}^2| \leqslant 7\,(\text{GeV/c})^2$ and have found that a dependence on $\tilde{q}^2$ of 10% per $1\,(\text{GeV/c})^2$ can be readily measured.

Note that the figures given for standard deviations in Table I include the statistical effects not only of the small e^+-e^- difference, but also of the large π^o photon background and of accidentals as well. In the previous work we determined both the π^0 production and the accidental rates, and hence we feel this calculation is sound. To give some idea of the relative size of the various contributions, the Compton, Bethe-Heitler, π^0, and accidental counts versus x are given in Table II.

When the information in Table I is summed over q^2 bins, as it would be if scaling in q^2 is found, then V(x) can be determined, and the accuracy of doing so is shown in Fig. 4. The V(x) assumed for the Monte Carlo is that deduced[7] from the electron scattering measurements, and assuming the quark charge is fractional. From the figure one sees that the assumed V(x) vanishes at large x, which is the reason our calculated errors become large there. The apparatus actually has appreciable sensitivity at large x.

Since V(x) is quite well determined, if one now integrates over the available range of x, one obtains an effect which is 25 standard deviations from zero, for fractional charge. This would provide a 4% statistical error in $\langle Q^3 \rangle$ and would, apart from the uncertainties due to the small x region discussed previously, provide an excellent charge determination. At the same time, if all the inelastic scattering events with $|q^2|>3$ were recorded, then in each $1(\mathrm{GeV/c})^2$ interval in $|q^2|$ between 3 and 10 we would have statistical errors $\lesssim 0.1\%$, presumably guaranteeing the first observation of a deviation from one-photon exchange e^+-e^- equality.

We would like to set up the experiment during the SLAC off time starting in the summer of 1977, the length of which is nicely matched to the task. When SLAC running commences again we would like about three months of 10-20 pps check-out time, since there are a lot of counters to get functioning and calibrated. Data running could then follow.

REFERENCES

1. D. L. Fancher, D. O. Caldwell, J. P. Cumalat, A. M. Eisner, T. P. McPharlin, R. J. Morrison, F. V. Murphy, and S. J. Yellin, Phys. Rev. Letters 37, 1323 (1976).
2. A. M. Eisner, D. O. Caldwell, J. P. Cumalat, B. N. Kendall, T. P. McPharlin, R. J. Morrison, and F. V. Murphy, Phys. Rev. Letters 33, 865 (1974).
3. D. O. Caldwell, A. M. Eisner, V. B. Elings, B. N. Kendall, T. P. McPharlin, R. J. Morrison, F. V. Murphy, and B. W. Worster, Phys. Rev. Letters 33, 868 (1974).
4. S. J. Brodsky, J. F. Gunion, and R. L. Jaffe, Phys. Rev. D6 2487 (1972).
5. M. S. Chanowitz, private communication (but to be published); some of the ideas about color detection below color threshold appear in M. S. Chanowitz, LBL-5312 (1976).
6. R. J. Morrison, submitted to Nuclear Physics (1976).
7. R. Blankenbecler, et al. SLAC PUB 1531 (1975).

FIGURE CAPTIONS

Fig. 1 - Diagrams for the reaction $e^{\pm} + p \rightarrow e^{\pm} + p + \gamma +$ anything

Fig. 2 - Schematic experimental lay-out for the previous experiment (E-99).

Fig. 3 - A possible arrangement of lead glass blocks to carry out the proposed experiment.

Fig. 4 - The assumed V(x), based on electron scattering results, which is used in the Monte Carlo calculations. The errors shown are the statistical determination of V(x) which would result from 100 hours of full efficiency running on each polarity in the proposed experiment.

Table I - Number of Standard Deviations of the e^+-e^- Difference in Bins of x and $|q^2|$ [in $(GeV/c)^2$]

$\|q^2\|\backslash x$	0.1-0.2	0.2-0.3	0.3-0.4	0.4-0.5	0.5-0.6	0.6-0.7	0.7-0.8
1-2	7.6	12.6	10.4	7.6	4.8	2.3	1.5
2-3	0.3	5.4	7.3	6.1	5.0	3.0	1.6
3-5	0	1.7	3.9	4.9	4.3	2.8	1.5

Table II - Counts for Various Processes at One Polarity Versus x

Type\x	0.1-0.2	0.2-0.3	0.3-0.4	0.4-0.5	0.5-0.6	0.6-0.7	0.7-0.8
Compton	1359	3650	2402	1088	491	146	40
Bethe-Heitler	967	5250	6568	5469	5625	2081	1068
π^0 γ's	36876	121734	91869	51401	27721	12788	4215
Accidentals	1011	2236	1513	675	611	195	394

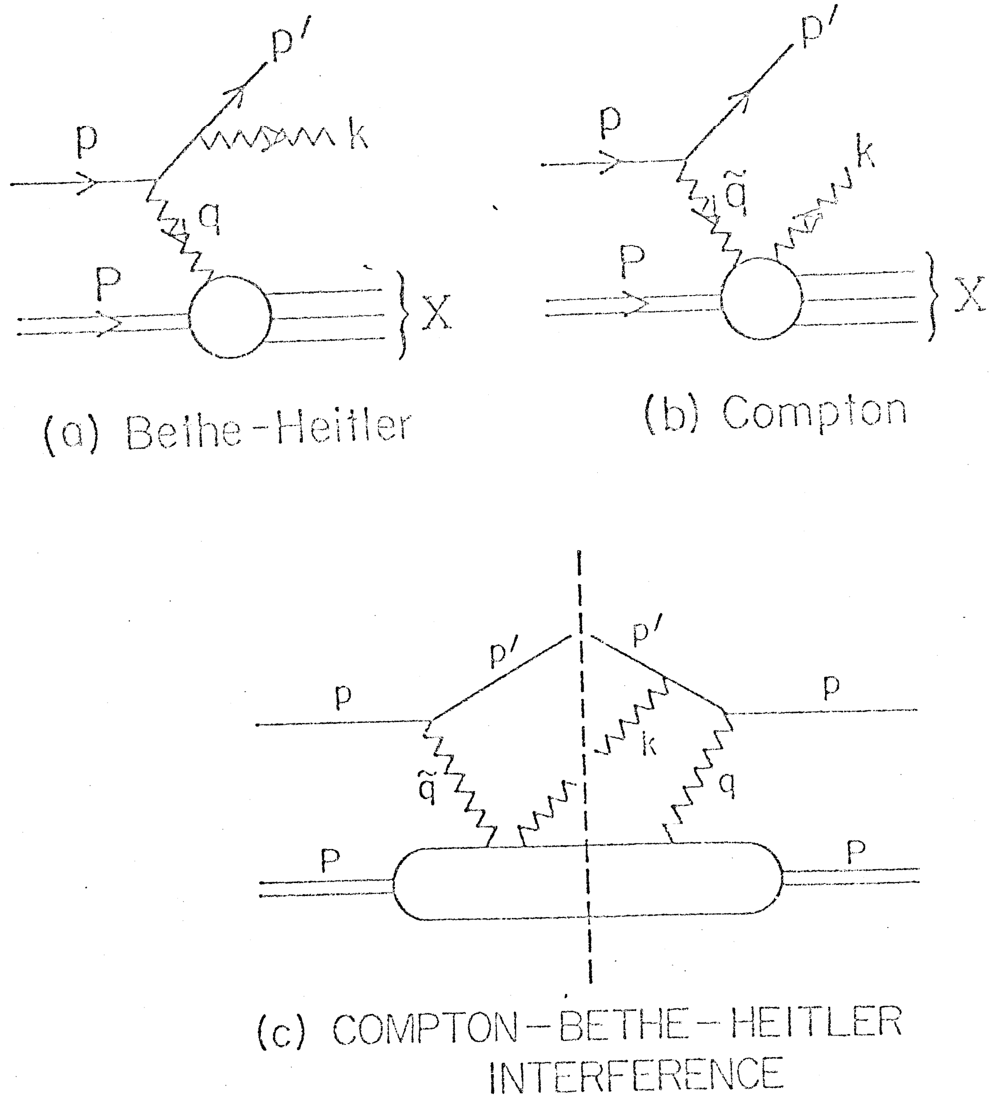
p
p′
k
q
P
X
(a) Bethe-Heitler
p
p′
$\tilde{q}$
k
P
X
(b) Compton
p′
p′
p
p
k
$\tilde{q}$
q
P
P
(c) COMPTON – BETHE – HEITLER
INTERFERENCE

Fig. 1

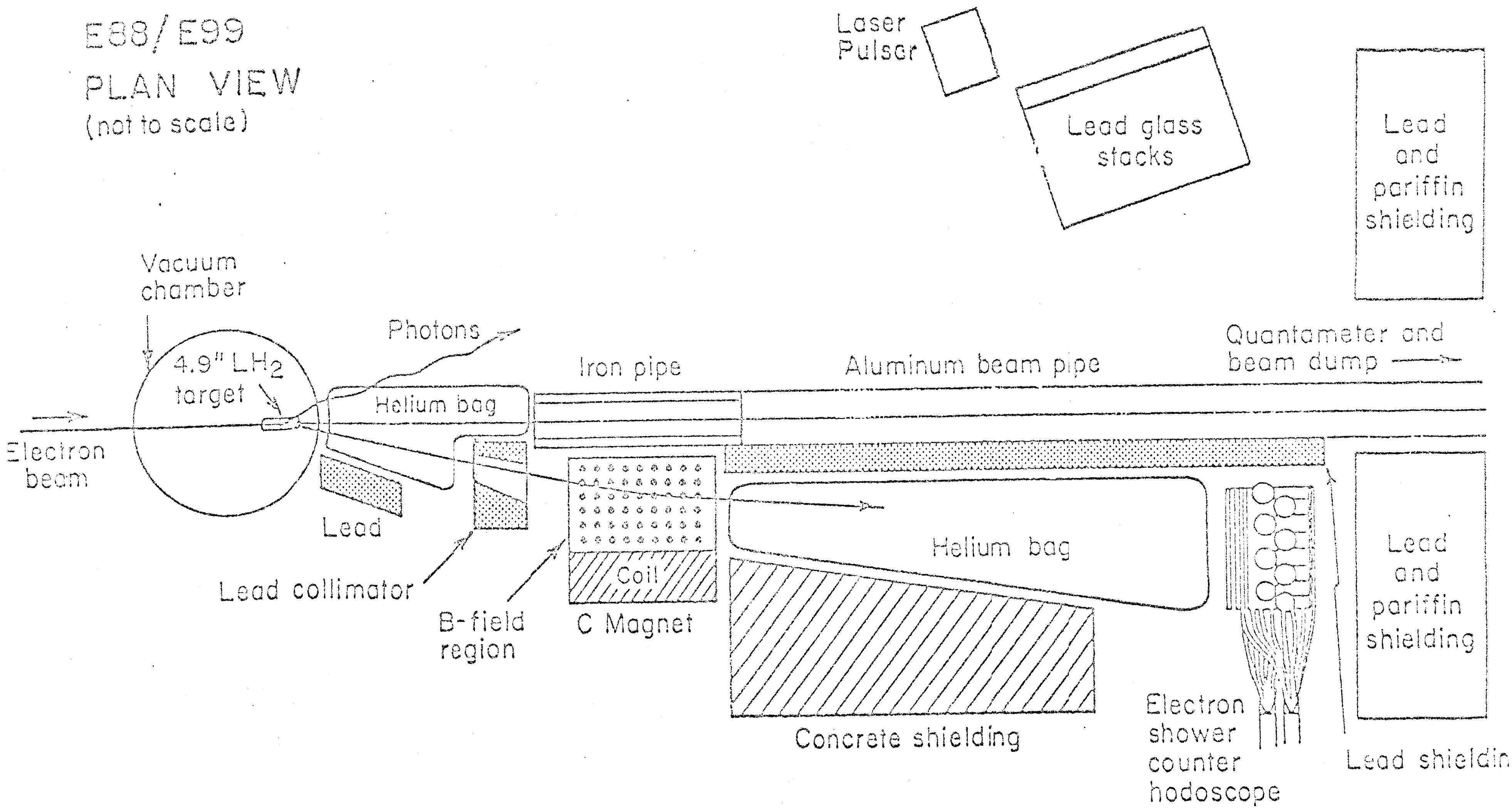

E88/E99
PLAN VIEW
(not to scale)
Laser
Pulser
Lead glass
stacks
Lead
and
pariffin
shielding
Vacuum
chamber
Photons
4.9" LH_2
target
Iron pipe
Aluminum beam pipe
Quantameter and
beam dump
Electron
beam
Helium bag
Lead
Lead collimator
B-field
region
Coil
C Magnet
Helium bag
Lead
and
pariffin
shielding
Concrete shielding
Electron
shower
counter
hodoscope
Lead shielding

Fig. 2

IDEALIZED ARRANGEMENT OF LEAD GLASS BLOCKS

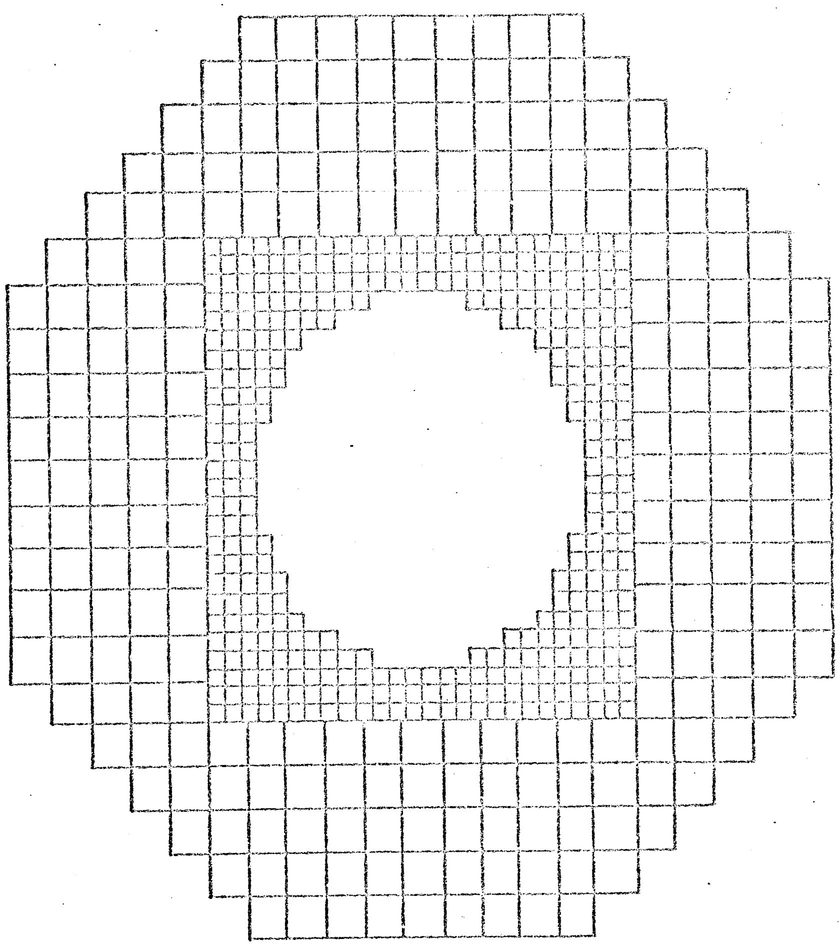

Fig. 3

SLAC Proposal No. E-124
April 1976

A Three-Photon Measurement of Parton Charge and Search for Color

Submitted by

University of California at Santa Barbara

D. O. Caldwell, A. M. Eisner, R. J. Morrison, and S. J. Yellin

April 1976

I. INTRODUCTION

The UCSB group has almost finished analyzing the results of a 200-hour trial (E-99) of an experiment which could in principle (1) provide a crucial test of the parton model, (2) determine whether partons have fractional or integral charge, and (3) check on the existence of "color". The limited statistics of E-99 preclude achieving these goals, but the results do demonstrate that the effect sought, a difference between $e^- + p \rightarrow e^- + \gamma$ + anything and $e^+ + p \rightarrow e^+ + \gamma$ + anything, does exist, consistent in kinematic behavior with the predictions of Brodsky, Gunion, and Jaffe.[1.] Furthermore, the magnitude of the effect is correct, giving a charge value roughly in the range expected.

Given this tantalizing result, as well as some others which will be mentioned below, we feel it is now essential to do the full experiment. This means not only having considerably more accelerator time, but also using apparatus with greatly increased solid angle. Since we also wish to reduce other errors and to profit by our experience, the apparatus needs to be somewhat more complex than before. At this time we feel we understand very well what is required, and we propose here one solution to these requirements, although we may not yet have achieved the optimum experimental design for the various available SLAC magnets and beams.

An auxiliary result which is of intrinsic interest, but which is also essential to the information on the parton model, parton charge, and the existence of color, is the comparison of electron and positron deep inelastic scattering. Over a range of $1<|q^2|<3$ $(GeV/c)^2$ and $2 < \nu < 10$ GeV we found $e^+ + p \rightarrow e^+ +$ anything/$e^- + p \rightarrow e^- +$ anything $= 1.0063 \pm 0.0029$. The lack of two-photon exchange effects to this level of accuracy is perhaps surprising, but in addition this result has two consequences for the main experiment: (1) two-photon interference effects cannot be responsible for the difference (of the order of 10%) we observe in the real photon production channel, and (2) this provides proof of no experimental biases in the e^+ and e^- detection which could affect the difference we observe in γ production.

In the proposed experiment we would obtain simultaneously with the photon production data an even more accurate comparison of e^+ and e^- deep inelastic scattering. In addition to the obvious improvement in statistics, we can also reduce the largest systematic error, which is the reproducibility of the e^+ and e^- beam positions, by installing a split ion chamber. The planned range of q^2 covered will also be increased by a factor of at least two.

Another experiment which can be performed simultaneously is π^0 electroproduction. At present we are still analyzing the results of such an experiment (E-88) and do not yet know which areas of the physics will require further looking into, although it is clear that the much bigger photon detector (300 counters instead of 88) will provide a far more efficient means of observing π^0's. At present there is controversial information (which bears on the structure of the photon) on whether the slope with transverse momentum of the π^0 electroproduction cross section changes with q^2, and it may be necessary to settle this issue with the new experiment.

II. THEORETICAL BACKGROUND

Brodsky, Gunion, and Jaffe[1] suggested that a difference could arise between the e^+ and e^- cross sections for deep inelastic electroproduction of photons from an interference between the Bethe-Heitler bremsstrahlung amplitude and the virtual Compton amplitude. These two processes are shown in Fig. 1. If the proton is considered to be made of partons, it is seen from these diagrams that one photon interacts with a parton in the Bethe-Heitler case and two photons interact with a parton in the Compton case, so that in taking the square, the interference term (Fig. 1c) is effectively a three-photon interaction with the parton. The interference or difference term then has odd charge conjugation and depends on the cube of the parton's charge.

Specifically, the difference of the positron and electron cross sections in the deep inelastic region determines a structure function

$$V(x) = \sum_a \lambda_a^3 U_a(x), \quad (1)$$

where $U_a(x)$ is the probability of finding a parton of type "a" with charge λ_a and fraction x of the proton's momentum in an infinite momentum rest frame. Note that V(x) depends on only one (x) of the six kinematic variables needed to specify the process. This scaling with x alone provides a very stringent test of the parton model and checking just this feature would be sufficient justification for the experiment.

Furthermore the measured V(x) determines $U_a(x)$, which has been sought in inelastic electron, muon, and neutrino experiments. In principle the present experiment is the cleanest way to determine the valence quark part of $U_a(x)$. Because of the odd charge conjugation there are no Pomeron contributions arising from the quark-antiquark sea in this process. Thus this experiment ought to shed further light on the behavior of valence quarks, provided V(x) scaling is observed.

If one could measure over all x values from 0 to 1, then the parton charge could be determined without any knowledge of $U_a(x)$ by using an exact sum rule. The point is that $Q=\int_0^1 dx \sum_a \lambda_a U_a(x)$, $Y = \int_0^1 dx \sum_a y_a U_a(x)$, and $B = \int_0^1 dx \sum_a b_a U_a(x)$ are the charge, hypercharge, and baryon number of the target parton of interest, and because it has odd charge conjugation, λ_a^3 can be reduced to a linear combination of λ_a, y_a, and b_a. Thus the integral $\int_0^1 V(x)dx = \int_0^1 dx \sum_a \lambda_a^3 U_a(x)$ is determined just by quantum number conservation. If the parton charge is 0 or ±1, $\lambda_a^3 = \lambda_a$, so

$$\int_0^1 V(x)dx = Q = \begin{cases} 1 \text{ for protons} \\ 0 \text{ for neutrons} \end{cases}, \qquad (2)$$

and for fractionally charged quarks, $\lambda_a^3 = \frac{1}{3}\lambda_a + \frac{2}{9} b_a$, so

$$\int_0^1 V(x)dx = \frac{1}{3} Q + \frac{2}{9} B = \begin{cases} 5/9 \text{ for protons} \\ 2/9 \text{ for neutrons} \end{cases}. \qquad (3)$$

Note that an even charge conjugation process, such as inelastic electron scattering, does not lead to an exact sum rule for the charge. Furthermore, if neutral gluons are present, the inexact sum rules obtained give an erroneously low charge value. The three-photon process considered here is completely insensitive to the presence of gluons.

Recently Chanowitz[2] has added an exciting new reason for doing this experiment, the detection of "color". Below the color threshold the electromagnetic current would display only color singlet interactions, and the standard quark-partons would show fractional charge. However, in some two-photon processes where the current comes in as the square, it is possible to have projected out a color octet piece. This results in

$$\int_0^1 V(x)dx = 7/9, \tag{4}$$

for fractionally charged quarks below the color threshold. This, then, is a specific and very important reason for doing this experiment at SLAC energies.

To somewhat diminish this euphoric state, we have recently noted a problem with determining the sum rule, namely that a relatively large part of the contribution must come from the small x region, where there can be a Reggeon-exchange contribution with an integrable $x^{-\frac{1}{2}}$ singularity. One can obtain a limit on the contribution to $\int V(x)dx$ from the large x region by noting that

$$\nu W_2^{ep}(x) = x \sum_a \lambda_a^2 \, U_a(x) \tag{5}$$

and getting an upper bound from assuming that only the p (or up) quark contributes with its charge of + 2/3. Thus

$$\frac{2}{3} \int_{x_o}^{1} \frac{\nu}{x} W_2^{ep}(x)dx > \int_{x_o}^{1} V(x)dx. \qquad (6)$$

The measurable lower limit, x_o, depends on how small a value of q^2 (see Fig. 1) one can use and still get scaling, and only the experiment can determine that. However $x_o = 0.05$ is an absolute limit and $x_o = 0.1$ or possibly even 0.2 are more likely. At these values of x_o the unmeasured contribution to $\int V(x)dx$ is appreciable, if the whole integral is equal to 5/9. Thus there are two ways to do the experiment: (1) measure to sufficiently small x so that the data can be extrapolated to x = 0, knowing the $x^{-\frac{1}{2}}$ dependence, which is fortunately possible because there can be no x^{-1} Pomeron contribution, or (2) use the larger x region where $U_a(x)$ has been well determined, and in effect take a ratio of experimental results. The inelastic scattering results (eq. 5) depend on λ^2, and the difference experiment (eq. 1) depends on λ^3, so the ratio determines λ. This comparison could even be extended down to moderately small x by correcting for the small Pomeron contribution to eq. 5. Obviously both approaches would be used, but the success of the first depends on getting scaling to small enough x so that the trend of V(x) is well enough established to make a meaningful extrapolation, and there is no way of guaranteeing the accuracy of that procedure at this stage, if partons have fractional charge. If the charge is integral, there is not such a large contribution at small x, and in any case it will be possible to show (method 2) that the bound of eq. 5 is exceeded for fractionally-charged quarks. ~~a right-hand side of 5/9, and perhaps even for 7/9~~. Thus this otherwise unfortunate development would then provide a powerful way of proving that the charges are integral.

III. PREVIOUS EXPERIMENT (E-99)

Using apparatus (Fig. 2) originally designed for an experiment (E-88) on deep inelastic π^0 production, the UCSB group used 200 hours of accelerator time to check out and try the three-photon experiment. As can be seen from the figure, there was a stack of 88 lead glass counters (of 2½" x 2½" cross section) on one side of the 13.5-GeV e^+ or e^- beam, and a recoil electron detector on the other side. Electrons emerging from the hydrogen target passed through a magnetic field (and in most cases through thin hodoscoped scintillators) and then into a hodoscoped lead and scintillator shower detector. Since the target was small, the production angle, momentum, and energy were determined. This redundancy aided in rejecting pions. Pion contamination was determined directly by reversing the polarity of the bending magnet, a result which was checked by placing lead in front of the electron detector to attenuate the $e^\pm$ contribution with the correct magnet polarity.

Although a wider range was covered in E-88 by having a higher beam energy and moving the detectors, in E-99 we used a single position and detected electrons such as to give virtual photons of $|q^2|$ from 1 to 3 $(\mathrm{GeV}/c)^2$ and ν from 2 to 10 GeV. Interleaved

e^+ and e^- data were collected in equal amounts at three beam intensities (3×10^7, 5×10^7, and 7×10^7 e's/pulse), so that any rate-dependent effects could be monitored. This did not produce any important systematic errors in even the e^+-e^- inelastic scattering difference, nor did beam halo, beam diameter differences, beam angle error, magnetic field differences, quantameter errors, magnetic effects on phototubes, or high-energy δ-rays. The only systematic effects of importance were from pion contamination (discussed above) and from beam positioning errors. Both of these can be improved considerably next time.

For the photon detection experiment, all photons in time coincidence with a suitable electron and having an energy greater than 4 GeV had their pulse heights and arrival times recorded. With this information, it was relatively straightforward to make good corrections for accidental coincidences, although in principle if one were careful (as we were) to use the same beam intensities, these should subtract out in the e^+-e^- difference. Where the difference subtraction was really important was in eliminating the background from $\pi^0 \rightarrow 2\gamma$ decays. That this subtraction was being done correctly could be checked by measuring simultaneously the amount of π^0 production by analyzing those cases in which both photons had sufficient energy to be counted. It is important to note that <u>all</u> spurious hadronic processes (even the decay of presently unknown particles) must subtract out in this difference.

The result of the e^+ and e^- deep inelastic scattering comparison has been given above. Although that difference was less than 1% we did observe a difference in the channel in which an energetic photon was produced, getting $\frac{e^+ \to \gamma}{e^- \to \gamma} = 1.09 \pm 0.03$. In principle the mean cube of the parton charge could then be determined through integrating over V(x), which is given by

$$V(x) = \frac{\sigma_+ - \sigma_-}{\pi^2 \alpha^3 s(-q^2)\,|T_{int}|^2} \qquad (7)$$

where $\sigma_+ = \frac{d^6\sigma(e^+p \to e^+\gamma X)}{\frac{d^3p'}{p_o}\,\frac{d^3k}{k_o}}$ and $\sigma_- = \frac{d^6\sigma(e^-p \to e^-\gamma X)}{\frac{d^3p'}{p_o}\,\frac{d^3k}{k_o}}$, and where the various kinematic quantities are defined in Fig. 1 (with the subscript 0 indicating the energy part of the corresponding four-momentum), and $|T_{int}|^2$ is a known electrodynamic function arising from the interference of the Bethe-Heitler and Compton amplitudes. However, the small x problem discussed in the previous section makes the charge determination model dependent, because the data neither goes to very small x nor has good enough statistics. At this time it is safest to say that the charge is of roughly the right size, which in itself is rather remarkable, because unless the proton has point-like constituents there is no known reason for this result to occur. Also impressive is the fact that this difference term is supposed to change sign in different kinematic regions, and our data are consistent with that behavior.

IV. DIFFERENCES BETWEEN THE PREVIOUS AND PROPOSED EXPERIMENTS

In the proposed experiment we should like to get nearly an order of magnitude improvement in statistics, as well as to reduce some potential systematic errors. We shall discuss here in a general way how these aims are to be carried out. The systematic effects will be discussed in connection with each part of the apparatus. As to the improvement in statistics, we are requesting 1000 hours, which will provide more than a factor of 5 over our previous 200 hours, since much of the latter was used in the inevitable start-up and check-out processes. Furthermore, the polarity switching was quite wasteful of time, especially at first, and that can be improved considerably. It is presently planned to improve the effective solid angle by a factor of 4 or 5. In addition, the increased beam energy (20 GeV instead of 13.5, making available a larger deep inelastic region) and beam intensity (since magnetic sweeping will be provided in front of the photon detector) should give another factor of about 3.

Considering now each part of the experiment, we note first the intention to use a higher beam energy to get a more extensive deep inelastic region and to permit measurements to smaller x. We have been informed that positrons can be made farther up the accelerator without major effort for the intensities we need (around 10^8/pulse). To keep the beams the same, the positron source is used also as an electron source. Our previous beam was sufficiently halo-free, but if we work farther out in the Perl Group area, as is discussed below, the beam can be made even cleaner. For the e^+-e^- deep inelastic scattering comparison we want this time to reduce the error due to beam position reproducibility, and this can be done if the beam is steered with a split ion chamber.

The hydrogen target would again be about 5" in length, since this gave us a tolerable 10% empty target contribution (which essentially subtracts out in the difference anyway), and it provides close enough to a point source to not dominate the errors in determining the kinematic quantities. There is a possibility if we improve the electron detector sufficiently that halving the target length would be desirable, but we have observed before that the beam can then be doubled in intensity to give the same background rates.

The main limitation in beam rate before came from the pile-up of small pulses in the photon counters, and hence this time we should like to provide magnetic sweeping ahead of the lead glass detectors, which of course look directly at the target. The best solution for doing this is to use two C magnets of opposite polarity, one for sweeping and the other for $e^{\pm}$ analysis, but with a field-free region between for the beam. Unless one or both magnets can be borrowed elsewhere, the cost of this arrangement at SLAC appears from first estimates to be too high. If the experiment is approved, we shall continue to look into this alternative, but for purposes of this proposal we are assuming that it will be necessary to use a single H magnet with a superconducting "straw" for the beam. Several such magnets are presently available at SLAC. The best of these would be the 100D40, but again the cost of moving this magnet or of bringing the beam to it appears to be too great. The readily movable magnets, the 72D36 and the 40D48, do not seem quite suitable, since the former would not provide enough sweeping and the latter does not have quite enough vertical acceptance. Furthermore, both of these would probably require our operating once again in End Station B, where because of LASS and the Hybrid Chamber operation we would need a shielded enclave for access, and again first estimates indicate high cost for that. The cheapest alternative at present appears to be using the 54" Dia. Spark Chamber Magnet of the Perl Group. The area would require more shielding and costs for this are just starting to be looked into, but present guesses are that this will involve the least work for SLAC. While it is probably not the best alternative for the experiment, we shall assume that choice here and show that the experiment done that way is feasible. We are by no means convinced that this is the optimum way to proceed and would, upon approval of the experiment, expend much effort in looking at other alternatives.

With a photon collimator and a stack 30" wide at 300" from the target, the 26 kg·m of the 54" magnet will sweep out charged particles of 8 GeV/c or lower. Because of the $\pi^{\pm}$ asymmetry, it will probably be necessary to provide some additional pion rejection in the outer edges of the stack, although our short blocks have themselves very good pion rejection.

The photon detector would consist of 300 blocks of lead glass of 2½" x 2½" cross section, like our previous 88 blocks. In a subsequent experiment at FNAL we have made great improvements in our laser light-pulser system for maintaining the calibration. While the basic calibration could again be done with an e^+ beam (and auxiliary steering magnets), we could make use this time with such a big stack of a continuous calibration also on the π^0 mass.

On the electron side we would again use the redundancy of both an energy and a momentum determination. This redundancy rejects pions and provides a better determination of the kinematic quantities; for example, we should like to measure x to ±10%. This time we wish to improve the accuracy of the momentum determination by utilizing proportional wire chambers. To take the rate it is necessary that the chambers not see the target, and hence the idea is to provide a shield on the electron side of the beam, take electrons of 7° to 11° and bend these back toward the beam into chambers behind the shield. The chambers, which would probably be those presently available from the Perl Group, would be located in two groups at 200" and 300" from the target. Behind the chambers we should like to use lead glass, although the financing of that is not clear at this time. Previously we used lead and scintillator, which could again be used, but we would like to have the improved energy resolution of the lead glass, and the help of the glass mosaic in rejecting accidental tracks in the chambers. On this side of the beam in addition to direct e^+ beam calibrations and the laser pulser system, the wires and magnet would provide a continuous calibration check.

V. RATES AND TIME

With the set-up described above -- and we reiterate that this is not an optimum arrangement -- we could get in 1000 hours at a nominal 180 pps nearly two orders of magnitude more data than in the previous experiment, and we feel that this is likely to be sufficient to achieve the aims described in the first section.

Besides the lack of firmness in the temporarily chosen experimental lay-out, there are other uncertainties in the quantity of data to be obtained. In general one wants $|q^2|$, $|\tilde{q}^2|$, and $|\tilde{q}^2 - q^2|$ large (see Fig. 1), but it is unclear how large. This can only be determined from the scaling check, and the quantity of data is determined particularly by the requirement on $|q^2|$. The signal-to-background ratio is best for high photon energies, making it hard to get to large $|q^2|$. While large k_o (photon energy) avoids π^o backgrounds, we may be able to reduce this problem somewhat by pairing γ's and hence throwing out π^o's. The π^o (and other backgrounds) of course subtract out in the difference, but they add greatly to the statistical error because the signal-to-background ratio is so small.

One should not weight all kinematic regions equally, but just to give an approximate idea of the quantity of data to be obtained from this set-up, if we lump together all the data for electron angles of 7^o to 11^o, ν of 6 to 14 GeV, and k_o of 6 to 11 GeV, then we get a difference signal of about 8000 after subtraction from a background of about 88,000, which gives about a 4 or 5% error, instead of the present error of ~30%.

Although we have now had considerable experience with this measurement and even more experience with the techniques involved, the experiment proposed here is a rather large undertaking for the UCSB group. At present we have, in addition to students, four faculty members, one postdoctoral research associate, and another such position we hope to fill soon. We have talked with potential collaborators and have had some enthusiastic responses. It may be that these negotiations will have been settled by the time this proposal is presented, as indeed we hope that some of the other information in it will be firmer by that time. Obviously the time at which the experiment would be ready depends on the extent of the help obtained, but a rough guess is summer of 1977.

REFERENCES

1. S. J. Brodsky, J. F. Gunion, and R. L. Jaffe, Phys. Rev. D6 2487 (1972).
2. M. S. Chanowitz, private communication (but to be published); some of the ideas about color detection below color threshold appear in M. S. Chanowitz, LBL-4237 (1975).

FIGURE CAPTIONS

Fig. 1 - Diagrams for the reaction $e^{\pm} + p \to e^{\pm} + p + \gamma$ + anything

Fig. 2 - Schematic experimental lay-out for the previous experiment (E-99).

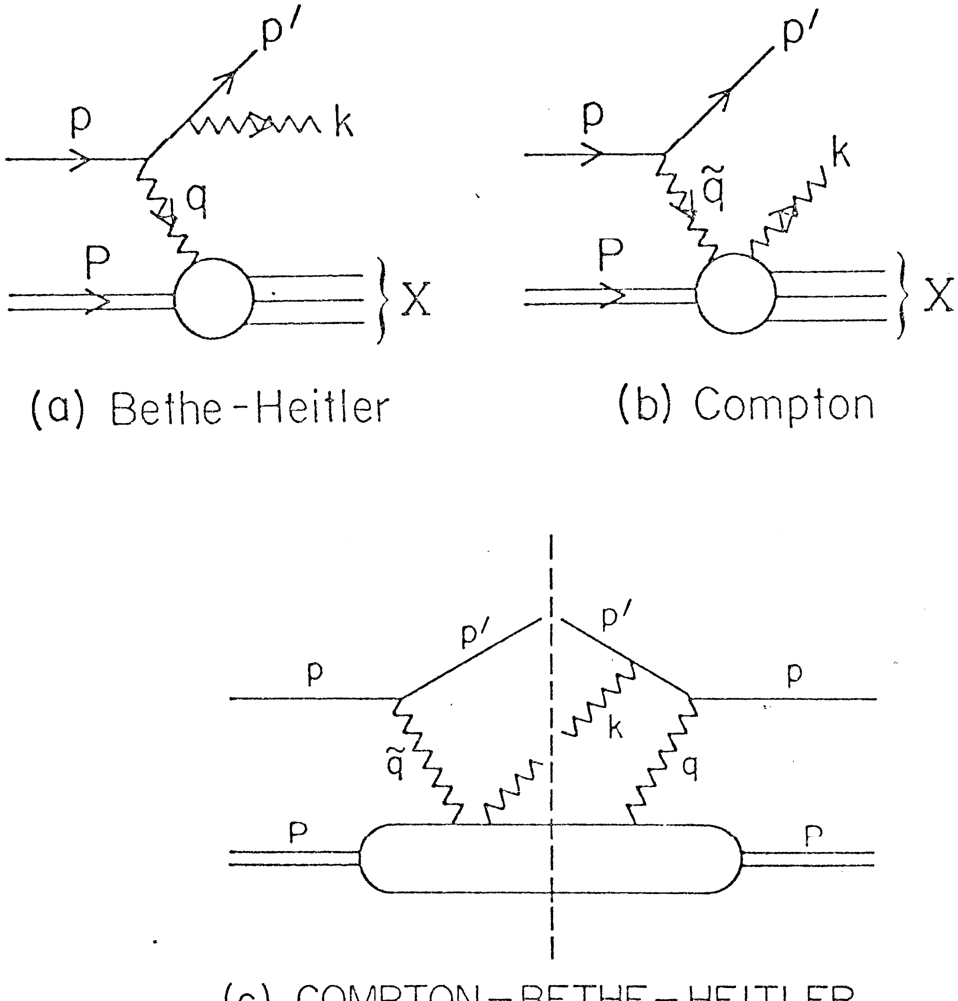

(a) Bethe-Heitler (b) Compton

(c) COMPTON-BETHE-HEITLER INTERFERENCE

Fig. 1

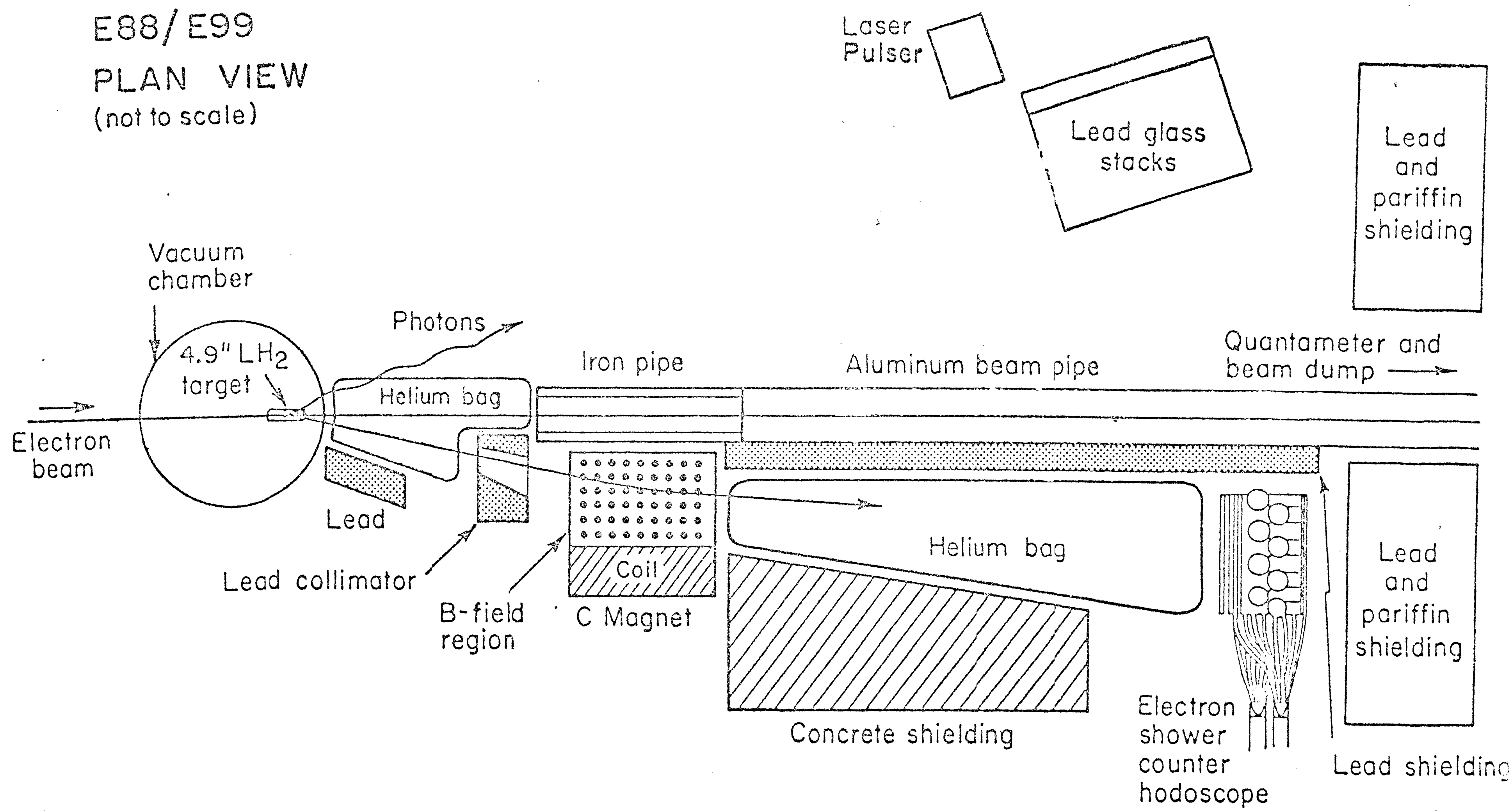
E88/E99
PLAN VIEW
(not to scale)
Laser
Pulser
Lead glass
stacks
Lead
and
pariffin
shielding
Vacuum
chamber
Photons
4.9" LH_2
target
Electron
beam
Helium bag
Iron pipe
Aluminum beam pipe
Quantameter and
beam dump
Lead
Lead collimator
B-field
region
Coil
C Magnet
Helium bag
Concrete shielding
Electron
shower
counter
hodoscope
Lead
and
pariffin
shielding
Lead shielding

Fig. 2